


# Effects of Low-Intensity Pulsed Ultrasound on the Migration and Homing of Human Amnion-Derived Mesenchymal Stem Cells to Ovaries in Rats With Premature Ovarian Insufficiency

Cell Transplantation  
Volume 31: 1–19  
© The Author(s) 2022  
Article reuse guidelines:  
sagepub.com/journals-permissions  
DOI: 10.1177/09636897221129171  
journals.sagepub.com/home/cll  


Li Ling<sup>1\*</sup> , Jiying Hou<sup>1\*</sup>, Yan Wang<sup>2</sup>, Han Shu<sup>1</sup>, and Yubin Huang<sup>1</sup>

## Abstract

Premature ovarian insufficiency (POI) can cause multiple sequelae and is currently incurable. Mesenchymal stem cell (MSC) transplantation might provide an effective treatment method for POI. However, the clinical application of systemic MSC transplantation is limited by the low efficiency of cell homing to target tissue *in vivo*, including systemic MSC transplantation for POI treatment. Thus, exploration of methods to promote MSC homing is necessary. This study was to investigate the effects of low-intensity pulsed ultrasound (LIPUS) on the migration and homing of transplanted human amnion-derived MSCs (hAD-MSCs) to ovaries in rats with chemotherapy-induced POI. For LIPUS treatment, hAD-MSCs were exposed to LIPUS or sham irradiation. Chemokine receptor expressions in hAD-MSCs were detected by polymerase chain reaction (PCR), Western blot, and immunofluorescence assays. hAD-MSC migration was detected by wound healing and transwell migration assays. Cyclophosphamide-induced POI rat models were established to evaluate the effects of LIPUS on the homing of systemically transplanted hAD-MSCs to chemotherapy-induced POI ovaries *in vivo*. We found that hAD-MSCs expressed chemokine receptors. The LIPUS promoted the expression of chemokine receptors, especially CXCR4, in hAD-MSCs. SDF-1 induced hAD-MSC migration. The LIPUS promoted hAD-MSC migration induced by SDF-1 through SDF-1/CXCR4 axis. SDF-1 levels significantly increased in ovaries induced by chemotherapy in POI rats. Pretreating hAD-MSCs with LIPUS increased the number of hAD-MSCs homing to ovaries in rats with chemotherapy-induced POI to some extent. However, the difference was not significant. Both hAD-MSC and LIPUS-pretreated hAD-MSC transplantation reduced ovarian injuries and improved ovarian function in rats with chemotherapy-induced POI. CXCR4 antagonist significantly reduced the number of hAD-MSCs- and LIPUS-pretreated hAD-MSCs homing to POI ovaries, and further reduced their efficacy in POI treatment. According to these findings, pretreating MSCs with LIPUS before transplantation might provide a novel, convenient, and safe technique to explore for improving the homing of systemically transplanted MSCs to target tissue.

## Keywords

premature ovarian insufficiency (POI), human amnion-derived mesenchymal stem cells (hAD-MSCs), low-intensity pulsed ultrasound (LIPUS), chemokine receptor, migration, home

## Introduction

Premature ovarian insufficiency (POI) is defined by loss of ovarian activity before the age of 40 years in women<sup>1</sup>. The pathological characterization of POI is amenorrhea or oligomenorrhea for at least 4 months with raised follicle-stimulating hormone (FSH, >25 mIU/ml) and low estradiol (E2) levels<sup>1</sup>. The prevalence of POI is about 1% in women<sup>1</sup>. The POI can be caused by various factors, especially the wide use of chemotherapy. Untreated POI causes multiple sequelae, including infertility, increased risk of fracture and cardiovascular disease, depression, and genitourinary symptoms<sup>1</sup>.

<sup>1</sup> Department of Obstetrics and Gynecology, The Second Affiliated Hospital of Chongqing Medical University, Chongqing, China

<sup>2</sup> State Key Laboratory of Ultrasound Engineering in Medicine Co-founded by Chongqing and the Ministry of Science and Technology, Chongqing Key Laboratory of Biomedical Engineering, College of Biomedical Engineering, Chongqing Medical University, Chongqing, China

\* Both authors are the co- first authors of this article.

Submitted: April 3, 2022. Revised: July 31, 2022. Accepted: September 9, 2022.

### Corresponding Author:

Li Ling, Department of Obstetrics and Gynecology, The Second Affiliated Hospital of Chongqing Medical University, No. 74, Linjiang Road, Chongqing 400010, China.

Email: 304869@hospital.cqmu.edu.cn



The POI is irreversible and currently incurable. Today, mesenchymal stem cell (MSC) transplantation has been the focus of a regime of emerging therapeutics to regenerate damaged tissue and treat refractory disease<sup>2</sup>. Regenerative medicine studies have suggested that MSC transplantation might provide an effective treatment method for POI<sup>3,4</sup>.

Human amnion-derived mesenchymal stem cells (hAD-MSCs) have been proved to have the features of MSCs<sup>5,6</sup>. Moreover, the procedure used to obtain hAD-MSCs is noninvasive and out of ethical debate, and hAD-MSCs have low immunogenicity permitting allogenic or xenogeneic transplantation<sup>5,7,8</sup>. These advantages make hAD-MSCs a promising *seed cell* for tissue engineering and regenerative medicine. Our previous studies have demonstrated that systemic intravenous transplantation of hAD-MSCs can partly reduce ovarian injury and improve ovarian function in rats with chemotherapy-induced POI<sup>8</sup>. However, the homing rate of systemically transplanted hAD-MSCs in POI ovaries was low, which might limit the efficiency of MSCs for POI treatment<sup>9</sup>.

At present, local transplantation of MSCs is usually invasive and the potential for minimally invasive delivery of MSCs via systemic infusion is still of particular interest<sup>2</sup>. Systemic intravenous transplantation of stem cells is the least invasive method and most commonly used<sup>2</sup>. Studies have been performed to explore the systemic transplantation of MSCs to treat a variety of diseases<sup>2</sup>. However, a critical barrier to the effective implementation of MSC therapy is the inability to target these cells to aim tissue with high efficiency<sup>2</sup>, which causes low homing rate of MSCs and further influences their efficacy in the treatment of diseases<sup>10–12</sup>.

Cell migration is an important part of cell homing<sup>13,14</sup>. Exogenous MSC homing is known as a process where transplanted MSCs are recruited from the peripheral bloodstream to injured or pathological tissue<sup>2,12</sup>. Although it is expected that higher numbers of systemically infused MSCs should result in higher numbers of homed MSCs and better functional outcomes, there may be a plateau beyond which additionally delivered cells may not improve the outcome<sup>2,15</sup>, and even lead to microvascular occlusions<sup>16</sup>. Previous studies have shown that although MSC transplantation has a good application prospect in the treatment of POI, low homing and engraftment rates of MSCs affect its efficacy and clinical application to some extent<sup>17,18</sup>. Our preliminary studies also found that the homing rate of the systemic transplantation of hAD-MSCs to treat POI was low<sup>9</sup> and we further attempted to optimize the transplantation protocol through choosing higher numbers of cells or/and different timing for transplantation. However, differences in the extent of cell homing and ovarian functional improvement were not apparent. Thus, exploration of methods to promote MSC homing is necessary. If there are some ways to increase MSC homing rate *in vivo*, the efficacy of MSC transplantation in POI treatment might be enhanced.

Any improvement of existing cell-based therapeutic approaches will depend on a better understanding of the interaction of stem cells with the environment that leads to homing and tissue integration<sup>19</sup>. However, molecular mechanisms that direct the migration and homing of MSCs are only partially understood<sup>19</sup>. Some studies have proved that the interaction between chemokines in tissue and chemokine receptors on MSCs mediates the migration and homing of MSCs to injured tissue<sup>20–23</sup>. Studies have found that MSCs express some specific chemokine receptors that may mediate aspects of MSC migration and homing, that is, CXC chemokine receptor 4 (CXCR4), CXCR6, C-C motif chemokine receptor 1 (CCR1), CCR2, CCR3, CCR7, and C-X3-C motif chemokine receptor 1 (CX3CR1)<sup>10,19,24,25</sup>. Studies have demonstrated that<sup>25</sup> the chemokine receptor repertoire of human bone marrow-derived mesenchymal stem cells (BM-MSCs) determined their migratory activity and homing capacity, and enhancing the migratory potential of MSCs by modulating their chemokine receptors and chemokine–chemokine receptor interaction may be a powerful way to enhance homing capacity of stem cells after transplantation and be instrumental for harnessing the therapeutic potential of MSCs. Thus, various techniques were conducted to enhance the expression of chemokine receptor on MSCs for promoting the homing of exogenous transplanted MSCs<sup>10,26–28</sup>. Although these preconditioning strategies might provide potential methods for enhancing the homing of MSCs to specific tissue, there are still some limitations<sup>2,10,29–32</sup>. The key limitations of these approaches are the protocol complexity and the requirement for viral transduction or DNA transfection, which may lead to significant changes in the properties of MSCs<sup>2,10,22,29–32</sup>. Thus, exploration of new methods to promote the homing of transplanted MSCs is necessary.

Low-intensity pulsed ultrasound (LIPUS) is a kind of mechanical wave, of which studies have been conducted with frequencies between 45 kHz and 3 MHz, intensity levels between 5 and 500 mW/cm<sup>2</sup>, duty cycles from 20% to 50%, and pulse repetition rates from 100 Hz to 1 kHz<sup>33–35</sup>. It has been reported that LIPUS is able to be transmitted into cells and generate a series of biochemical events at cellular level<sup>33,36,37</sup>. MSCs have been reported to have the ability to respond to physical stimuli<sup>36,38</sup>. Some studies have found that LIPUS can promote the expression of chemokine receptors, CXCR4 and CCR2, in MSCs<sup>24,39</sup>. Several preliminary studies have suggested that LIPUS can affect MSCs and promote MSC migration and homing<sup>14,24</sup>. However, whether LIPUS can promote the expression of chemokine receptors in hAD-MSCs, and further promote hAD-MSC migration and homing, is still unknown.

In this study, whether LIPUS could promote the expression of chemokine receptors in hAD-MSCs, whether LIPUS could influence the migration of hAD-MSCs, and whether pretreating hAD-MSCs with LIPUS could increase the number of hAD-MSCs homing to the ovaries in rats with chemotherapy-induced POI and further improve the efficacy of MSC transplantation in POI treatment were investigated.

## Materials and Methods

The experimental protocols were in compliance with the Helsinki Declaration and approved by the Ethics Committee of the Second Affiliated Hospital of Chongqing Medical University.

### Reagents

Fetal bovine serum (FBS) was purchased from Gibco Co (Grand Island, NY, USA). Cell Counting Kit-8 (CCK-8), Aging-related  $\beta$ -galactosidase (SA- $\beta$ -Gal) staining kit, RIPA lysis buffer, and BeyoECL Plus kit were purchased from Beyotime Institute of Biotechnology (Haimen, China). 5-ethynyl-2'-deoxyuridine (EdU) was purchased from Ribobio Co Ltd (Guangzhou, China). CCR3, CCR4, CCR10, and CXCR4 antibodies were purchased from Novus Biologicals (Littleton, CO, USA). p21, p16, and  $\beta$ -actin antibodies were purchased from Proteintech Co (Wuhan, China). Repressor/activator protein 1 (Rap1) and NADH dehydrogenase (ubiquinone) iron-sulfur protein 6 (Ndufs6) antibodies were purchased from Thermo Fisher Scientific Co (Waltham, MA, USA). TRIzol Reagent was purchased from Invitrogen (Carlsbad, CA, USA). ReverTra Ace-, first strand cDNA Synthesis Kit was purchased from TOYOBO Life Science (Shanghai, China). Stromal cell-derived factor-1 (SDF-1), anti-Müllerian hormone (AMH), and E2 and FSH ELISA kits were purchased from USCN Life Science (Wuhan, China). AMD3100 was purchased from MedChemExpress (Monmouth Junction, NJ, USA). 2-(4-amidinophenyl)-6-indolecarbamide dihydrochloride (DAPI) was purchased from Boster Biological Technology Co Ltd (Wuhan, China). DyLight549 was purchased from Abbkine Scientific Co Ltd (Wuhan, China). All other chemicals were purchased from Sigma-Aldrich Co (St. Louis, MO, USA).

### Isolation, Culture, and Identification of hAD-MSCs

Primary hAD-MSCs were isolated, cultured, and identified according to our previous protocols<sup>6</sup>. hAD-MSCs were isolated from the amnions of term placentas. Term placentas from healthy donors (n = 28) were collected from patients who received cesarean sections at the Second Affiliated Hospital of Chongqing Medical University, China. About an average of 3.08  $\times$  10<sup>6</sup> hAD-MSCs were yielded from an amnion<sup>6</sup>. The cell growth and senescence were compared between the fifth passage (P5) of hAD-MSCs and the third passage (P3) of hAD-MSCs. P5 of hAD-MSCs was used for the subsequent experiments.

### LIPUS Treatment Protocol

The LIPUS exposure device was provided by Chongqing Haifu Medical Technology Co Ltd, Chongqing, China (Fig. 1A). The parameters of LIPUS device were set as follows according to our previous studies<sup>6,40</sup>: spatial-average temporal-average

intensity ( $I_{SATA}$ ), 30 mW/cm<sup>2</sup>; exposure time (ET), 30 min; frequency, 0.25 MHz; duty cycle, 20%; burst width sine wave, 200  $\mu$ s; pulse repetition frequency, 1 kHz. The device consisted of 6 transducers (diameter = 34.8 mm) in an array, which was specifically designed for 6-well culture plates. Cells can be placed on the transducers and get LIPUS treatment (Fig. 1B). Cells were divided into the control and LIPUS groups. Cells were exposed to LIPUS in the LIPUS group, while cells were exposed to sham irradiation (LIPUS generator was not switched on) in the control group.

### CCK-8 Assay

CCK-8 assay was used to detect cell viability according to the manufacturer's instructions. hAD-MSCs were cultured for 24 h and then exposed to sham irradiation or LIPUS for 5 days. The optical density (OD) value at 450 nm was measured every day after treatment using a plate reader (1510 model; Thermo Fisher Scientific Oy, Vantaa, Finland).

### SA-el; Thermo Fis

SA-el; Thermo Fis kit was used for staining according to the manufacturer's instructions. Senescent cells were stained blue. Cells were observed and imaged under an optical microscope (Olympus Corporation, Tokyo, Japan). The hAD-MSC senescence rate was defined as the ratio of SA-dGal-positive cells (blue cells) to total cells present in 200  $\times$  00lls (blue cells) to total cells present in ratio o

### EdU Assay

Cells were cultured for 24 h and then exposed to LIPUS or sham irradiation. EdU assay was used to detect cell proliferation at 24 h after treatment according to the manufacturer's instructions. Cells were observed and imaged under a fluorescent microscope (Olympus Corporation). The numbers of EdU and Hoechst33342-positive cells were counted. The hAD-MSC proliferation rate was defined as the ratio of EdU-positive cells to total Hoechst33342-positive cells.

### Flow Cytometry

Cells were treated as described in EdU assay. At 24 h after treatment, cells were collected and incubated with annexin-V-FITC and PI. The hAD-MSC apoptosis rate was detected by flow cytometry.

### Transwell Migration Assay

A cell migration model *in vitro* was constructed by transwell chamber (Corning, Corning, NY, USA) composed of a membrane filter with 8  $\mu$ m diameter pores suspended in a six-well plate according to the manufacturer's instructions. hAD-MSCs were randomly divided into the control 1, control 2, LIPUS, LIPUS + inhibitor and inhibitor groups. hAD-MSCs,

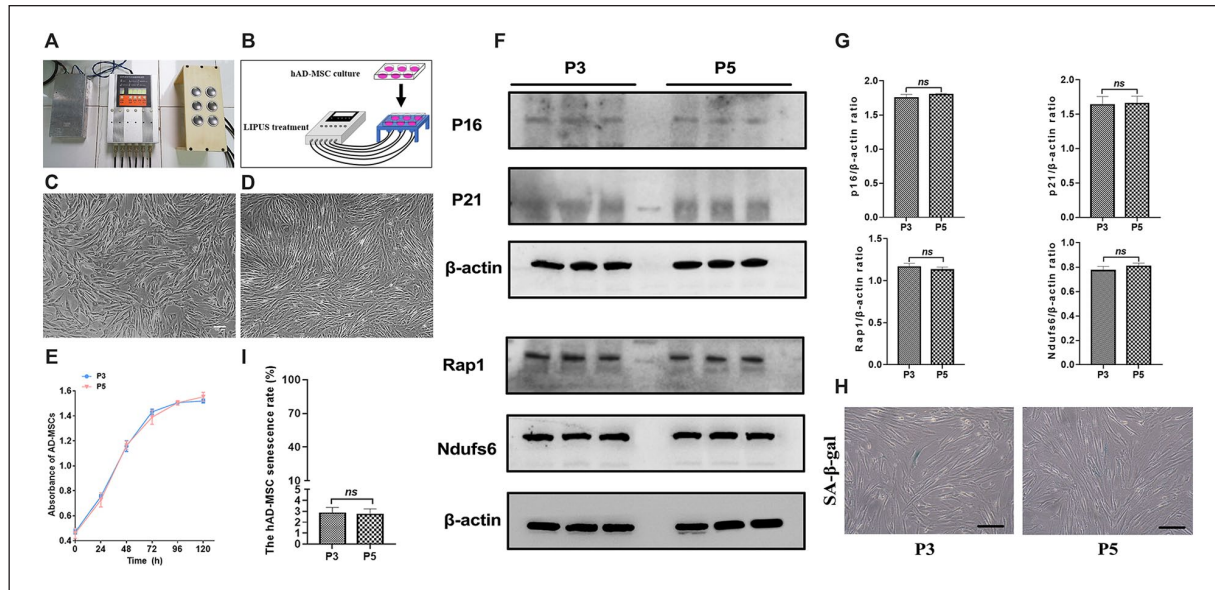


**Figure 1.** Schematic diagram of LIPUS treatment and characterization of hAD-MSCs. (A) LIPUS device. (B) Schematic diagram of LIPUS treatment for hAD-MSCs. (C, D) The cell morphology of hAD-MSCs was observed at (C) 3 and (D) 5 days after culture ( $100\times$  culture (hology of hAD-MSCs was o the fifth passage (P5) and the third passage (P3) were measured using CCK-8 assay ( $n = 6$ ). (F, G) The expressions of p16, p21, Ndufs6 and Rap1 in hAD-MSCs at P5 and P3 were analyzed (F) and compared (G) using Western blot. (H, I) Senescent cells of hAD-MSCs at P5 and P3 were detected (H) and compared (I) using SA- $\beta$ -Gal staining ( $n = 3$ ). Independent-samples  $t$  test was used for two-group comparisons. CCK-8: cell counting kit-8; hAD-MSCs: human amnion-derived mesenchymal stem cells; LIPUS: low-intensity pulsed ultrasound; NS: not significant. \* $P < 0.05$ ; \*\* $P < 0.01$ . Scale bars =  $100\ \mu\text{m}$ ; scale bars =  $200\ \mu\text{m}$ .

exposed to sham irradiation for 5 days, were placed into the upper chamber in the control 1, control 2, and inhibitor groups, while LIPUS-pretreated hAD-MSCs, exposed to LIPUS for 5 days, were placed into the upper chamber in the LIPUS and LIPUS + inhibitor groups. In these five groups, cells were placed in serum-free medium at a density of  $1 \times 10^5/\text{cm}^2$  into the upper chamber, and the lower chamber was filled with same medium containing 2% FBS. Moreover, chemokine SDF-1 (chemokine ligand for CXCR4) (100 ng/ml) was added into the lower chamber in the control-2, LIPUS, LIPUS + inhibitor and inhibitor groups, and AMD3100 (specific inhibitor of CXCR4) (44 nM) was additionally added into the upper chamber in the inhibitor and LIPUS + inhibitor groups. After 24 h, migration assays were terminated by retrieving the membrane filter from each group, and hAD-MSCs on the underside of the filter were stained with crystal violet staining solution and counted in six visual fields ( $200\times$ ) randomly chosen under microscope (Olympus Corporation).

### Wound Healing Assay

Wound healing assay was also performed to detect hAD-MSC migration. hAD-MSCs were seeded in six-well plates and cultured to 100% confluence, wounds were made among the area of hAD-MSCs by scratching with a  $200\ \mu\text{l}$  pipette tip (three wounds per well). hAD-MSCs were

divided into the control-1, control-2, LIPUS, LIPUS + inhibitor and inhibitor groups. After that, the medium was replaced with low serum medium containing 2% FBS. AMD3100 (44 nM) was added into the medium in the inhibitor and LIPUS + inhibitor groups, and SDF-1 (100 ng/ml) was added into the medium in the control 2, LIPUS, LIPUS + inhibitor and inhibitor groups. Then, hAD-MSCs in the control 1, control 2, and inhibitor groups were exposed to sham irradiation, while hAD-MSCs in the LIPUS and LIPUS + inhibitor groups were exposed to LIPUS. The scratched and covered areas of each group were observed at 0 and 24 h after treatment, respectively, under an optical microscope (Olympus Corporation). The area of scratch was measured using Image J v1.42q software (National Institutes of Health, Bethesda, MD, USA). The area covered ratio of migration cells (ACRMC) was defined as (covered area / scratched area)  $\times 100\%$ .

### Reverse Transcriptional PCR

Primers used in the experiment were listed in Table 1. Total RNA was extracted using TRIzol Reagent. RNA sample was quantified and reverse transcribed into cDNA using the ReverTra Ace-erfirst strand cDNA Synthesis Kit. Electrophoresis of 10 octrophoresis of sis Kit. transcribed into cDNA usin120 V for 30 min on 1.5% agarose gel, and images were analyzed.  $\beta$ -actin was used as a positive control.

**Table 1.** Primer Sequences for Polymerase Chain Reaction.

Gene	Primer sequence 5'→3'	Amplification	Accession no.
CCR1	CCCCTGGTAGAAAG AAGATGAATG	261 bp	NM_001295.3
CCR2	GGGGAGGTGATGGAAGAACAG CCGCTGCTCATCATGGTCATC ATGGGATTGATGCAGCAGTGAG	269 bp	NM_001123041.3
CCR3	TGTGGCTATCCTTCTCTCTTC CAAGTGCCTGTGGAAGAAG	193 bp	NM_001164680.2
CCR4	TGCCGTGGTGGTCTCTTC ATGGGATTAAGGCAGCAGTGAAC	171 bp	NM_005508.5
CCR5	CGCCTTAGGTAATTATTCCAG CCCAAATTCAAAACAGTCTCAAG	192 bp	NM_000579.4
CCR7	TCCACAGACTCAAATGCTCAG CGGCAAGTGAGGGGATGAGTG	226 bp	NM_001301714.2
CCR9	TGCTGCTATACCATCATCATTAC GGGAAACTGAGACAAGACAAAGAC	114 bp	NM_001256369.2
CCR10	GCGCACACTTGGTCTCCGTC CGCCACCAGAGCCACCACG	293 bp	NM_016602.3
CXCR1	GGTGGATGAACAAAGAGAAAG GCTGCTTGTCTCGTTCCAC	133 bp	NM_000634.3
CXCR2	GGACTCCTCAAGATTCTAGCTATAC GGCCTCCTCTACTTCCTGTGAC	251 bp	NM_001168298.2
CXCR4	TCCTGCCTGGTATTGTCATCC CACCTTGCTTGATGATTTCC	196 bp	NM_001008540.2
CXCR5	AGGCCGAGAAGCAAGAAAGAAAC AAGGGAGTGAGGAGGGGACAAGC	213 bp	NM_001716.5
CXCR6	GGCCACCAGCATGTTCCAGTTATAG GCATTCCAAACCAGCCAGAGTG	164 bp	NM_001386435.1
CX3CR1	CACCCATCCTATCAGCCTGTCTC GCTGGAAAGGATGATCTCTATGTG	210 bp	NM_001171171.2
β-actin	ACCCCGTGTGCTGACCGAG TCCCGGCCAGCCAGGTCCA	250 bp	NM_001101.5

### Real-Time Quantitative PCR

Cells were cultured for 24 h and exposed to LIPUS or sham irradiation for 5 days. Then, RNA samples were extracted, quantified, and reverse transcribed into cDNA. Real-time quantitative PCR (RT-qPCR) was performed using a CFX96 Real-Time PCR Detection System (Bio-Rad, Hercules, CA, USA) with SYBR Green Real-Time PCR Master Mix (TOYOBO Life Science). Target gene expression was determined using the  $2^{-\Delta\Delta C_t}$  method. β-actin was used as internal reference.

### Western Blot

Cells were treated as described in RT-qPCR. The proteins in hAD-MSCs were extracted, quantified, separated by sodium dodecyl-sulfate polyacrylamide gel electrophoresis (SDS-PAGE), and subsequently electro-transferred to polyvinylidene difluoride (PVDF) membranes (Millipore, Billerica, MA, USA). After that, the membranes were incubated with specific primary antibodies for p16, p21, Ndufs6, Rap1, CCR3, CCR4,

CCR10, and CXCR4, and then the corresponding secondary antibodies. BeyoECL Plus kit was used for color development according to the manufacturer's instructions.

### Immunofluorescence Assay

Cells were treated as described in RT-qPCR. The cells were incubated with specific primary antibodies for CXCR4 followed by the secondary antibodies conjugated with DyLight549. The cells were counterstained with DAPI and imaged under a laser scanning confocal microscope (Nikon Corporation, Tokyo, Japan).

### Labeling and Tracking of hAD-MSCs

To track and locate the transplanted hAD-MSCs in rats, hAD-MSCs were prelabeled with PKH26 Red Fluorescent Cell Linker Kits according to our previous published protocols<sup>8</sup>. At 24 h after transplantation, ovaries and other organs were made into fresh sections. The sections were incubated with DAPI

and imaged under a laser scanning confocal microscope or a fluorescent microscope (all from Nikon Corporation).

The quantification of homing efficiency of hAD-MSCs within ovarian tissue is typically assessed by averaging the number of PKH26-labeled cells present in 800 $\times$  microscopic fields randomly chosen from per tissue sample under confocal microscope according to the protocol which has been published<sup>19</sup>.

### Animal Protocols

Female Sprague-Dawley (SD) rats aged 10 to 12 weeks were purchased from the Experimental Animal Center of Chongqing Medical University.

A total of 144 of female SD rats were randomly divided into six groups as follows: control, POI, hAD-MSCs, LIPUS + hAD-MSCs, hAD-MSCs + AMD3100, and LIPUS + hAD-MSCs + AMD3100 groups (n = 24 in each group). Rats were intraperitoneally injected with cyclophosphamide to establish the POI model in the POI, hAD-MSCs, LIPUS + hAD-MSCs, hAD-MSCs + AMD3100, and LIPUS + hAD-MSCs + AMD3100 groups according to our previous published protocols<sup>8</sup>. For the inhibitor treatment, hAD-MSCs were incubated with AMD3100 (44 nM) for 1 h before cell transplantation in the hAD-MSCs + AMD3100 and LIPUS + hAD-MSCs + AMD3100 groups. Then, at 24 h after chemotherapy, the rats from the hAD-MSCs and hAD-MSCs+AMD3100 groups were injected with  $4 \times 10^6$  hAD-MSCs (exposed to sham irradiation for 5 days), while the rats from the LIPUS + hAD-MSCs and LIPUS + hAD-MSCs+AMD3100 groups were injected with LIPUS-pretreated hAD-MSCs (exposed to LIPUS for 5 days), labeled with PKH-26, via the tail vein. At 24 h, 3 and 6 weeks after cell transplantation, six rats in each group were sacrificed under sodium pentobarbital anesthesia and samples were collected for the subsequent experiments.

Regular and irregular estrous cycles of rats in each group were recorded by vaginal smears observation as described in our previous published protocols<sup>8</sup>. Regular estrous cycles consist of four sequential stages as follows: proestrus, estrus, metestrus, and diestrus (Fig. 9D).

Mating trials was performed to detect reproductive capacity of female rats. Six female rats in each group were housed with fertile male rats at a ratio of 3:1 for 3 months from the eighth week after chemotherapy. Then, the number of offspring per rats in each group was recorded.

### Enzyme-Linked Immunosorbent Assay

The SDF-1 levels in the ovaries and serum of POI rats at 24 h after chemotherapy were detected by Enzyme-Linked Immunosorbent Assay (ELISA) kits according to the manufacturer OI rats at as

To detect the serum levels of AMH, FSH, and E2 of rats in each group, serum was collected at 0, 3, and 6 weeks after

cell transplantation and analyzed using ELISA kits according to the manufacturer previous I model

### Ovarian Morphology Analysis and Follicle Counts

Ten ovaries from each group were collected at 6 weeks after hAD-MSC transplantation. Ovaries were fixed, dehydrated, paraffin embedded, and cut into 5  $\mu$ a sections. The sections were stained with hematoxylin and eosin (HE). Ovarian morphology was observed by an optical microscope (Olympus Corporation). The follicles in ovaries were classified as below<sup>40,41</sup> (Fig. 9B) and counted as described previously<sup>40,42</sup>:

- Primordial follicle: A primary oocyte was surrounded by a single layer of flattened epithelial cells.
- Primary follicle: An enlarged primary oocyte was surrounded by unilaminar or multilaminar cuboidal (columnar) granulosa cells, with no liquor folliculi.
- Secondary follicle: A primary oocyte was surrounded by multilaminar cuboidal (columnar) granulosa cells, and liquor folliculi appeared in spaces between the granulosa cells.
- Preovulatory follicle: As the single antrum enlarged, the granulosa cells appeared as layers around the liquor folliculi, the layers became thinner, and cumulus oophorus formed.
- Atretic follicle: Atresia may occur at any stage of follicle development and it involved the death of granulosa cells and the oocyte.

### Statistical Analysis

For all assays, at least three independent experiments were performed. Statistical analysis of data was processed by SPSS 22.0 software (IBM, NY, USA). Data were presented as mean  $\pm$  standard deviation. One-way analysis of variance (ANOVA) and independent-samples *t* test were used for multiple-group and two-group comparisons, respectively. Statistical significance was set at  $P < 0.05$ .

## Results

### Characterization of hAD-MSCs

The isolated cells grew as adherent cultures, displayed a fibroblastic morphology, and were capable of forming colonies (Fig. 1C and D). These cells were identified according to our previous published protocols.<sup>6</sup> Our results demonstrate that the isolated cells have the common characteristics of multipotent MSCs and are identified as hAD-MSCs<sup>6</sup>.

To identify whether P5 of hAD-MSCs used in this study for transplantation underwent senescence, cell growth, expressions of senescence associated protein markers (p16, p21, Ndufs6 and Rap1)<sup>43-45</sup>, and cell senescence rates<sup>43</sup> were detected and compared between P5 and P3 of hAD-MSCs using CCK-8, Western blot, and SA- $\beta$ -Gal staining assays,

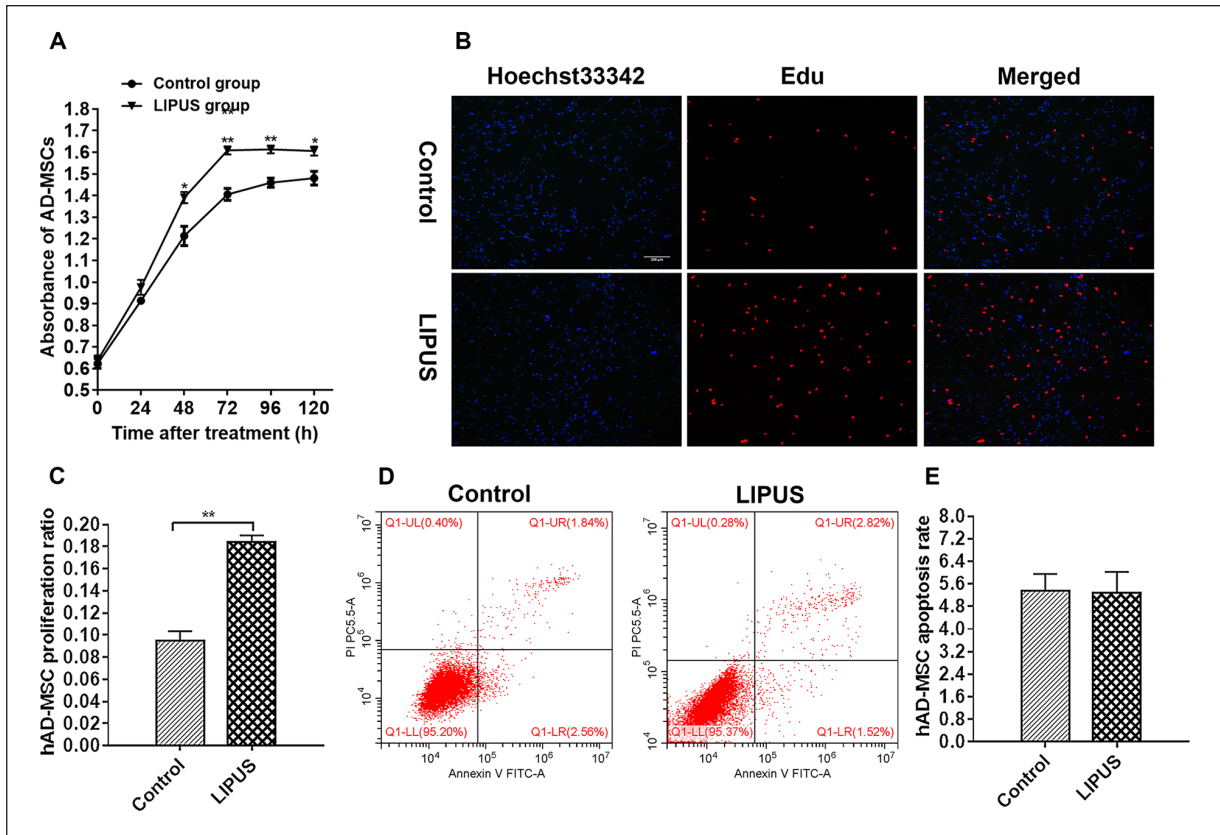


**Figure 2.** Effects of LIPUS on the viability, proliferation, and apoptosis of hAD-MSCs. (A) The growth curves of hAD-MSCs in the control and LIPUS groups were measured by CCK-8 assay ( $n = 6$ ). (B, C) The hAD-MSC proliferation ratios in the control and LIPUS groups were detected by Edu incorporation assay ( $100\times$  ( $n = 9$ )). (D, E) The hAD-MSC apoptosis rates in the control and LIPUS groups were detected by flow cytometry ( $n = 3$ ). Representative images are shown. Independent-samples *t* test was used for two-group comparisons. CCK-8: cell counting kit-8; hAD-MSCs: human amnion-derived mesenchymal stem cells; LIPUS: low-intensity pulsed ultrasound. \* $P < 0.05$ ; \*\* $P < 0.01$ . Scale bars =  $200\ \mu\text{m}$ .

respectively. It was found that there was no significant difference in the cell growth, expressions of p16, p21, Ndufs6 and Rap1, and hAD-MSC senescence rates between P3 and P5 of hAD-MSCs (Fig. 1E–I). These results demonstrate that the hAD-MSCs at P5 have not yet undergone significant senescence and hypofunction due to *in vitro* replication expansion and are able to be used for subsequent experiments.

### Effects of LIPUS on the Viability, Proliferation, and Apoptosis of hAD-MSCs

To explore the effects of LIPUS on the viability and growth of hAD-MSCs, CCK-8 assay was performed. The results showed that LIPUS significantly promoted the viability and growth of hAD-MSCs ( $P < 0.05$ , Fig. 2A). To further define the effects of LIPUS on the proliferation of hAD-MSCs, Edu incorporation assay was performed. The results showed the hAD-MSC proliferation ratio was significantly lower in the control group than in the LIPUS group ( $P < 0.01$ , Fig. 2B and C). Subsequently, to determine whether LIPUS affects the apoptosis of hAD-MSCs,

cell apoptosis rates were detected. The results showed that there was no significant difference in the hAD-MSC apoptosis rates between the control and LIPUS groups ( $P > 0.05$ , Fig. 2D and E). These results demonstrate that LIPUS can promote the viability and proliferation of hAD-MSCs and does not increase the apoptosis of hAD-MSCs, *in vitro*.

### The mRNA Expression Levels of Chemokine Receptors in hAD-MSCs

To explore the presence of chemokine receptors, which may be implicated in MSC migration and homing, in hAD-MSCs<sup>19,25</sup>, the mRNA expression levels of CCR1, CCR2, CCR3, CCR4, CCR5, CCR7, CCR9, CCR10, CXCR1, CXCR2, CXCR4, CXCR5, CXCR6 and CX3CR1 were detected by RT-PCR. The results showed that hAD-MSCs expressed CCR1, CCR2, CCR3, CCR4, CCR5, CCR7, CCR9, CCR10, CXCR1, CXCR2, CXCR4, CXCR5, CXCR6, and CX3CR1 (Fig. 3). CCR3, CCR4, CCR5,

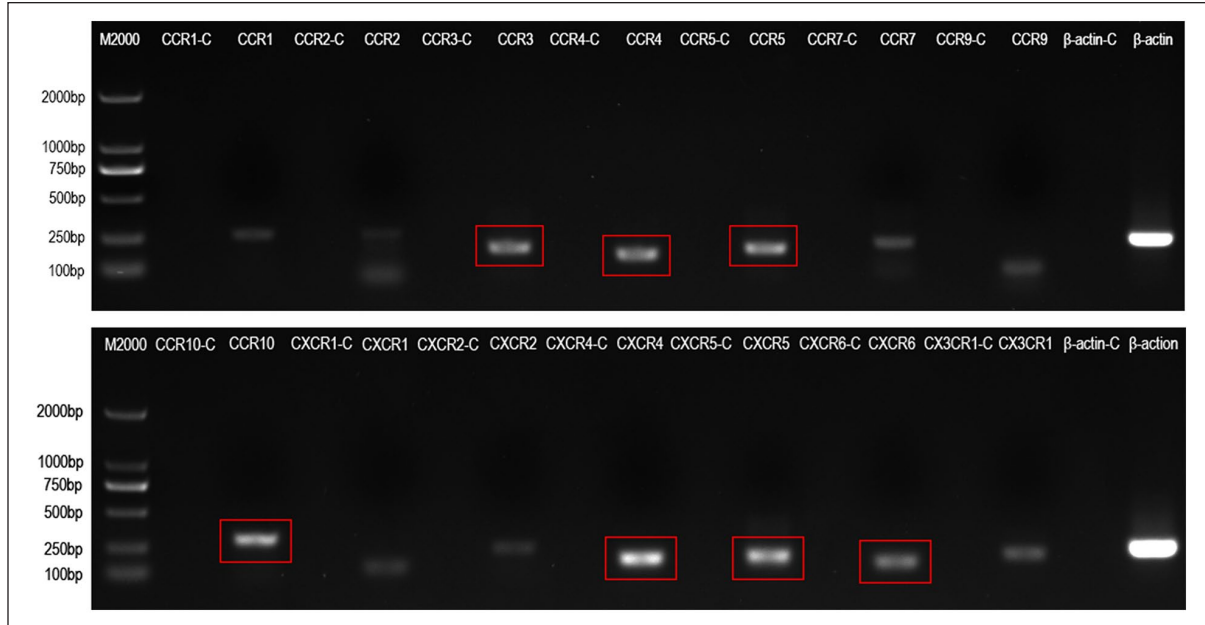


**Figure 3.** The mRNA expression levels of chemokine receptors in human amnion-derived mesenchymal stem cells (hAD-MSCs). The expressions of chemokine receptors in hAD-MSCs were detected by reverse transcriptional polymerase chain reaction. CCR3, CCR4, CCR5, CCR10, CXCR4, CXCR5 and CXCR6, having higher expressions in hAD-MSCs, were highlighted with red frame. CCR1-C, CCR2-C, CCR3-C, CCR4-C, CCR5-C, CCR7-C, CCR9-C, CCR10-C, CXCR1-C, CXCR2-C, CXCR4-C, CXCR5-C, CXCR6-C, CX3CR1-C, or  $\beta$ -actin-C is shown as a corresponding negative control, and  $\beta$ -actin is shown as a positive control. Three independent repeating experiments from three different donors were performed. Representative images from a donor are shown.

CCR10, CXCR4, CXCR5, and CXCR6, which had higher expressions (Fig. 3) in hAD-MSCs, were selected for the following experiments.

### LIPUS Promotes the Expression of Chemokine Receptors in hAD-MSCs

To determine whether LIPUS could promote the expression of chemokine receptors in hAD-MSCs, RT-qPCR, Western blot, and immunofluorescence assay were performed.

First, the effects of LIPUS on the mRNA expression levels of CCR3, CCR4, CCR5, CCR10, CXCR4, CXCR5, and CXCR6 in hAD-MSCs were detected by RT-qPCR. The results showed that the relative mRNA expression levels of CCR3, CCR4, CCR5, CCR10, CXCR4, CXCR5, and CXCR6 in hAD-MSCs were significantly higher in the LIPUS group than in the control group ( $P < 0.05$  and  $P < 0.01$ , Fig. 4A). CCR3, CCR4, CCR10, and CXCR4, of which the expression levels in hAD-MSCs were especially significantly increased by LIPUS treatment ( $P < 0.01$ , Fig. 4A), were selected for the following Western blot analysis.

Second, the effects of LIPUS on the protein expression levels of CCR3, CCR4, CCR10, and CXCR4 in hAD-MSCs were detected by Western blot analysis. The results showed that the protein expression levels of CCR4 and CXCR4 in hAD-MSCs were significantly higher in the LIPUS group than in the control group ( $P < 0.01$ , Fig. 4B and C). CXCR4, which has been found to play an important role in

the migration and homing of systemically transplanted hAD-MSCs to the ovaries of rats with chemotherapy-induced POI in our previous research<sup>46</sup>, was firstly selected to study in the following experiments.

Third, to further confirm whether LIPUS could promote CXCR4 expression in hAD-MSCs, immunofluorescence assay was performed. The results showed that the intensity of red fluorescent signals, which indicates the expression of CXCR4, was significantly higher in the LIPUS group than in the control group ( $P < 0.05$ , Fig. 4D and E).

These results demonstrate that LIPUS can promote the expression of CXCR4 in hAD-MSCs.

### Elevated SDF-1 Levels in Serum and Ovaries in POI Rats Induced by Chemotherapy

To explore whether chemotherapy induces the secretion of SDF-1 in ovaries of POI rats, SDF-1 concentrations in the serum and ovaries were measured in the control and POI groups. It was found that, compared with the control group, the levels of SDF-1 in the serum and ovaries were significantly increased in the POI group ( $P < 0.01$ , Fig. 5A and B).

These results demonstrate that chemotherapy induces the secretion of SDF-1 in ovaries of POI rats and the elevated SDF-1 levels in ovaries might attract transplanted hAD-MSCs and LIPUS-pretreated hAD-MSCs expressing CXCR4 *in vivo*. Moreover, LIPUS can promote CXCR4 expression in



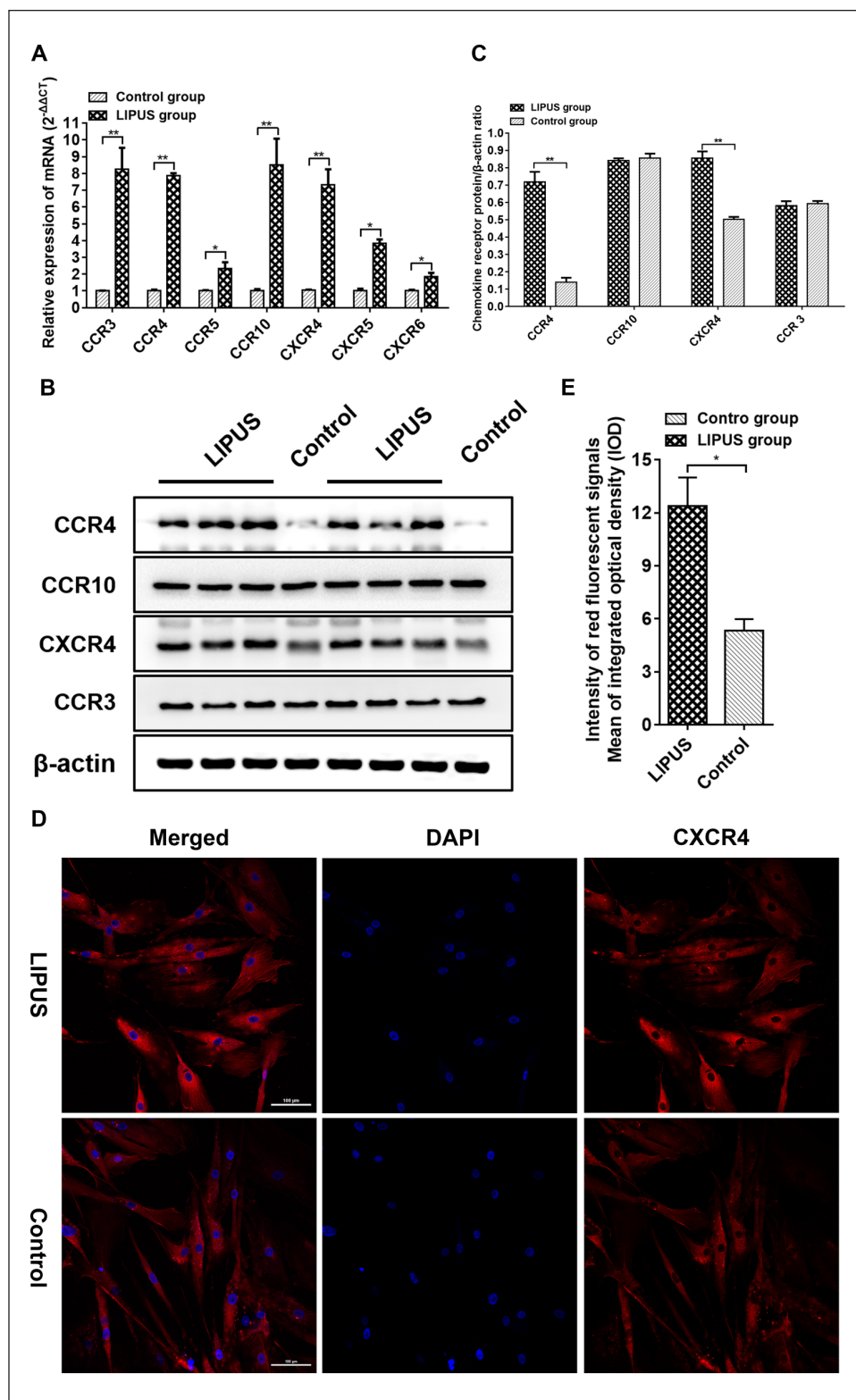


**Figure 4.** LIPUS promotes the expression of chemokine receptors in hAD-MSCs. (A) The effects of LIPUS on the mRNA expression levels of CCR3, CCR4, CCR5, CCR10, CXCR4, CXCR5 and CXCR6 in hAD-MSCs were detected by RT-qPCR. (B, C) The effects of LIPUS on the protein expression levels of CCR3, CCR4, CCR10, and CXCR4 in hAD-MSCs were detected by Western blot assay. (D, E) The effects of LIPUS on the protein expression of CXCR4 in hAD-MSCs were detected by immunofluorescence assay (200×00e = 6). Independent-samples *t* test was used for two-group comparisons. DAPI: 2-(4-amidinophenyl)-6-indolecarbamidine dihydrochloride; hAD-MSCs: human amnion-derived mesenchymal stem cells; IOD: integrated optical density; LIPUS: low-intensity pulsed ultrasound; RT-qPCR: real-time quantitative polymerase chain reaction. \**P* < 0.05 and \*\**P* < 0.01. Scale bars = 100 μm.

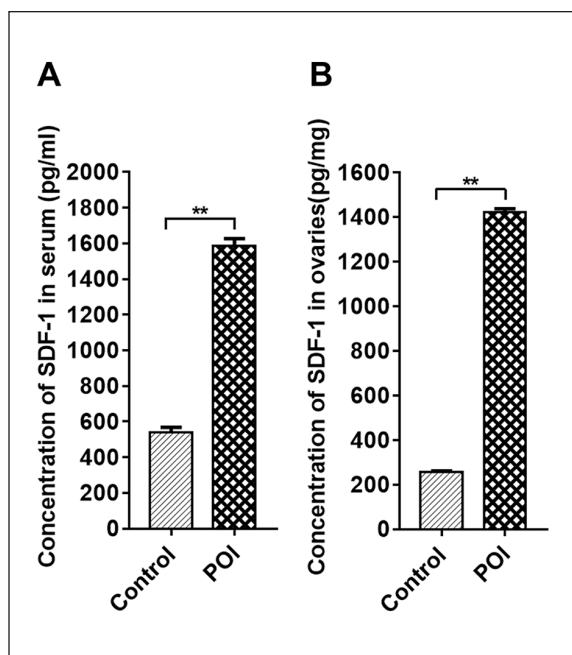


**Figure 5.** Elevated SDF-1 levels in the serum and ovaries in POI rats induced by chemotherapy. SDF-1 concentrations in the serum (A) and supernatant of homogenized ovarian tissue (B) in the control and POI groups were measured by ELISA assay. N = 6. Independent-samples t test was used for two-group comparisons. ELISA: enzyme-linked immunosorbent assay; POI: premature ovarian insufficiency; SDF-1: stromal cell-derived factor-1. \* $P < 0.05$ ; \*\* $P < 0.01$ .

hAD-MSCs, and LIPUS pretreatment on hAD-MSCs might be more advantageous to the migration and homing of hAD-MSCs to chemotherapy-induced POI ovaries.

### LIPUS Can Promote hAD-MSC Migration Induced by SDF-1 in Vitro

To examine whether LIPUS could promote hAD-MSC migration induced by SDF-1 *in vitro*, transwell migration and wound healing assays were performed.

The results showed that compared with the control 1 group, the number of hAD-MSCs passing through the membrane induced by SDF-1 was significantly greater in the control 2 group ( $P < 0.01$ , Fig. 6A and B). Compared with the control 2 group, the number of hAD-MSCs passing through the membrane induced by SDF-1 was significantly greater in the LIPUS group ( $P < 0.01$ , Fig. 6A and B). Moreover, compared with the LIPUS group, AMD3100 pretreatment significantly reduced the number of hAD-MSCs passing through the membrane promoted by LIPUS in the LIPUS + inhibitor group ( $P < 0.01$ , Fig. 6A and B).

On the contrary, the results showed that there was no significant difference in the size of the scratched area at 0 h after scratching between each group (Fig. 6C). At 24 h after scratching, compared with the control 2 group, ACRMC

induced by SDF-1 was significantly increased by LIPUS treatment in the LIPUS group ( $P < 0.01$ , Fig. 6C and D). Moreover, compared with the LIPUS group, AMD3100 pretreatment significantly reduced ACRMC promoted by LIPUS in the LIPUS + inhibitor group ( $P < 0.01$ , Fig. 6C and D).

These results demonstrate that SDF-1 can induce hAD-MSC migration *in vitro*. The pronounced stimulation of migration by SDF-1 suggests that the CXCR4 expressed in hAD-MSCs might be instrumental for targeted migration and homing of these cells. The LIPUS treatment can promote hAD-MSC migration induced by SDF-1 *in vitro*, which indicates that pretreating hAD-MSCs with LIPUS might increase the number of hAD-MSCs homing to the ovaries with elevated SDF-1 levels in rats with chemotherapy-induced POI.

### Effects of LIPUS on the Homing of hAD-MSCs to Chemotherapy-Induced POI Ovaries in Vivo

To confirm whether LIPUS pretreatment on hAD-MSCs is more advantageous to the homing of hAD-MSCs to chemotherapy-induced POI ovaries, hAD-MSCs and LIPUS-pretreated hAD-MSCs were transplanted into POI rats.

To track and locate the transplanted hAD-MSCs *in vivo*, hAD-MSCs were prelabeled with PKH26, which showed red fluorescence (Fig. 7A–C). The homing and location of transplanted PKH26-labeled hAD-MSCs in ovaries of POI rats were traced at 24 h after cell transplantation. The results showed that, PKH26-labeled cells, which showed red-dotted fluorescent signals, were recruited and located in the interstitium of POI ovaries after transplantation in the hAD-MSCs, LIPUS + hAD-MSCs, hAD-MSCs + AMD3100 and LIPUS + hAD-MSCs + AMD3100 groups (Fig. 7D). A quantitative assessment of the number of hAD-MSCs in ovaries revealed that ovaries in the hAD-MSCs, LIPUS + hAD-MSCs, hAD-MSCs + AMD3100, and LIPUS + hAD-MSCs + AMD3100 groups contained  $24.67 \pm 21.54$ ,  $27.67 \pm 23.78$ ,  $9.25 \pm 6.52$ , and  $11.08 \pm 9.83$  cells/microscopic field, respectively ( $n = 12$ , Fig. 7D and E). The intensity of red-dotted fluorescent signals and number of hAD-MSCs were higher in the LIPUS + hAD-MSCs group than in the hAD-MSCs group at 24 h after cell transplantation (Fig. 7D and E). However, the difference was not significant between these two groups ( $P > 0.05$ , Fig. 7D and E). The intensity of red-dotted fluorescent signals and number of hAD-MSCs were significantly lower in the hAD-MSCs + AMD3100 and LIPUS + hAD-MSCs + AMD3100 groups than in the hAD-MSCs and LIPUS + hAD-MSCs groups, respectively ( $P < 0.05$ , Fig. 7D and E). However, there was no significant difference between the hAD-MSCs + AMD3100 and LIPUS + hAD-MSCs + AMD3100 groups ( $P > 0.05$ , Fig. 7D and E). There were no red-dotted fluorescent signals in the control and POI groups (data not shown), which is consistent with our previous studies<sup>40</sup>.

Meanwhile, some red-dotted fluorescent signals were observed in the uteruses and spleens in the hAD-MSCs and LIPUS + hAD-MSCs groups (Fig. 8). Only a few red

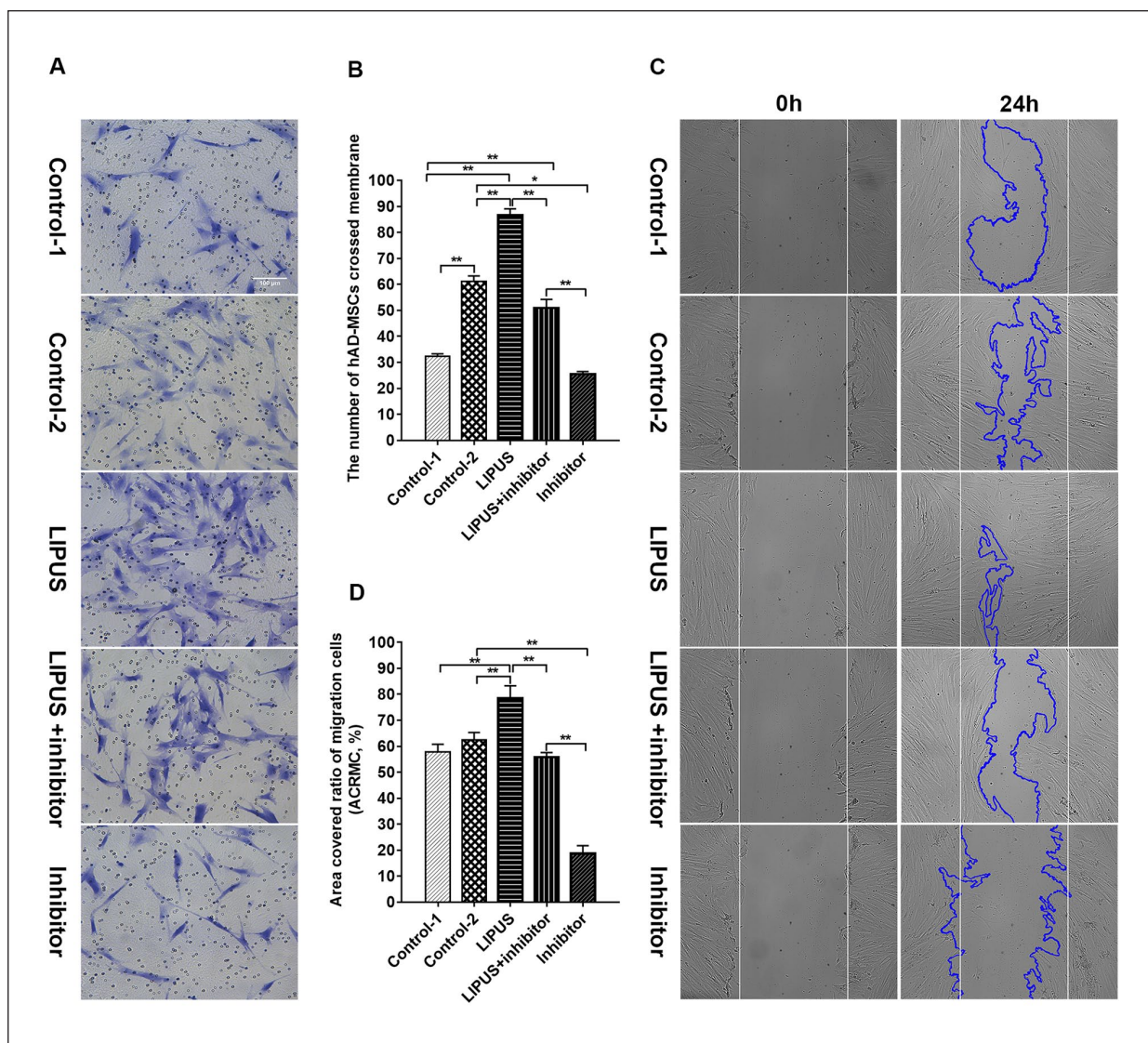


**Figure 6.** LIPUS promotes hAD-MSC migration induced by SDF-1 *in vitro*. The migration of hAD-MSCs was tested by transwell migration assay (A, B) ( $200\times 00\text{say}$  (A, B) (s was tes ( $100\times 00\text{sin}$  *in vitro*, in the control 1, control 2, LIPUS, LIPUS + inhibitor and inhibitor groups. Scratched areas and uncovered areas of hAD-MSCs were highlighted with white lines and blue lines, respectively. Representative images are shown. N = 6. One-way analysis of variance was used for multiple-group comparisons. ACRMC: area covered ratio of migration cells; hAD-MSCs: human amnion-derived mesenchymal stem cells; LIPUS: low-intensity pulsed ultrasound; SDF-1: stromal cell-derived factor-1. \* $P < 0.05$ ; \*\* $P < 0.01$ . Scale bars =  $100\ \mu\text{m}$ .

fluorescent signals were observed in the lungs, and no red fluorescent signals were observed in the kidneys, livers, hearts, and brains, in the hAD-MSCs and LIPUS + hAD-MSCs groups (Fig. 8). There was no significant difference between the two groups (Fig. 8).

These results demonstrate that ovaries of chemotherapy-induced POI rats are able to attract hAD-MSCs and LIPUS-pretreated hAD-MSCs, and CXCR4 expression in hAD-MSCs may play an important role in the homing of hAD-MSCs and LIPUS-pretreated hAD-MSCs to the POI ovaries. Pretreating hAD-MSCs with LIPUS can increase the number of hAD-MSCs homing to the ovaries of POI rats to some extent. However, the difference is not significant.

### Changes in Ovarian Injuries and Function After hAD-MSC and LIPUS-Pretreated hAD-MSC Transplantation in Rats With Chemotherapy-Induced POI

To investigate the effects of hAD-MSC and LIPUS-pretreated hAD-MSC transplantation on ovarian injuries and function in rats with chemotherapy-induced POI, ovarian histology, estrous cycles, sex hormone levels, and reproductive capacity of rats were analyzed.

The results showed that, compared with the control group, chemotherapy induced follicle loss, vascular damage, and tissue fibrosis in ovaries in the POI group (Fig. 9A–C), while

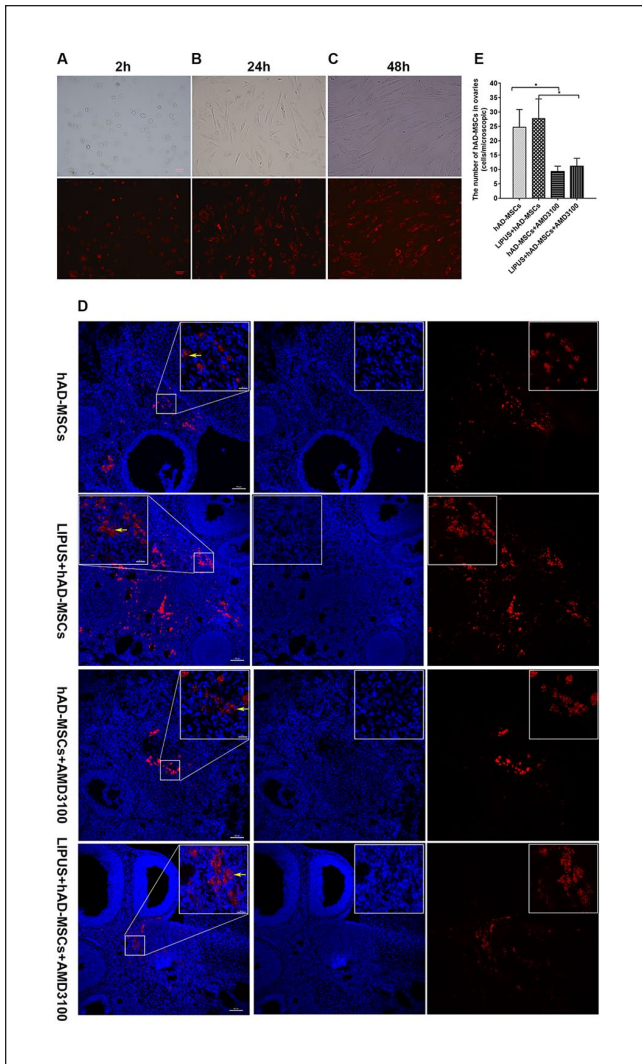


**Figure 7.** Effects of LIPUS on hAD-MSC homing to chemotherapy-induced POI ovaries *in vivo*. (A–C) The morphology of hAD-MSCs was observed under fluorescent microscope at (A) 2 h, (B) 24 h, and (C) 48 h after being labeled with PKH26 ( $100\times 0026$  (being labeled with MSCs was observed under fluorescent microscope at (A) at not shown), which is consistent with our 24 h after cell transplantation in the hAD-MSCs, LIPUS + hAD-MSCs, hAD-MSCs + AMD3100 and LIPUS + hAD-MSCs + AMD3100 groups by confocal microscopy analysis (D) ( $100\times$  and  $800\times 00d$  SCs + AMD3100 groups by confocal microscopy analysis (D) (microfour groups (E) ( $n = 12$ ). Representative images are shown. One-way analysis of variance was used for multiple-group comparisons. hAD-MSCs: human amnion-derived mesenchymal stem cells; LIPUS: low-intensity pulsed ultrasound; POI: premature ovarian insufficiency. \* $P < 0.05$ . The yellow arrows indicate transplanted hAD-MSCs. Scale bars =  $100\ \mu\text{m}$ ; scale bars =  $20\ \mu\text{m}$ .

compared with the POI group, hAD-MSC and LIPUS-pretreated hAD-MSC transplantation reduced follicle loss, vascular damage, and tissue fibrosis in the hAD-MSCs, LIPUS + hAD-MSCs, hAD-MSCs + AMD3100 and LIPUS

+ hAD-MSCs + AMD3100 groups (Fig. 9A–C). Compared with the control group, the number of primordial and growth follicles was significantly lower in the POI group ( $P < 0.05$ , Fig. 9A–C), while compared with the POI group, the number of primordial and growth follicles was significantly greater in the hAD-MSCs, LIPUS + hAD-MSCs, hAD-MSCs + AMD3100, and LIPUS + hAD-MSCs + AMD3100 groups ( $P < 0.05$ , Fig. 9A–C). Moreover, compared with the hAD-MSCs group, the number of primordial follicles was significantly lower in the hAD-MSCs + AMD3100 group ( $P < 0.05$ , Fig. 9A–C), while compared with the LIPUS + hAD-MSCs group, the number of primordial follicles was significantly lower in the LIPUS + hAD-MSCs + AMD3100 group ( $P < 0.05$ , Fig. 9A–C).

One hundred percent of rats in the POI group had irregular estrous cycles from the third week after chemotherapy (Fig. 9D and E). Compared with the POI group, the percentages of rats with irregular estrous cycles decreased in the hAD-MSCs, LIPUS + hAD-MSCs, hAD-MSCs + AMD3100 and LIPUS + hAD-MSCs + AMD3100 groups from the third week after hAD-MSC transplantation (Fig. 9D and E). Compared with the hAD-MSCs and LIPUS + hAD-MSCs groups, the percentages of rats with irregular estrous cycles increased in the hAD-MSCs + AMD3100 and LIPUS + hAD-MSCs + AMD3100 groups from the third week after hAD-MSC transplantation (Fig. 9D and E).

Compared with the control group, the AMH and E2 levels were significantly lower, while the FSH level was significantly higher after chemotherapy in the POI group ( $P < 0.05$ , Fig. 9F–H). Compared with the POI group, the AMH and E2 levels were significantly higher, while the FSH levels were significantly lower in the hAD-MSCs, LIPUS + hAD-MSCs, hAD-MSCs + AMD3100, and LIPUS + hAD-MSCs + AMD3100 groups, from the third week after hAD-MSC transplantation ( $P < 0.05$ , Fig. 9F–H). Moreover, compared with the hAD-MSCs group, the AMH level was significantly lower in the hAD-MSCs + AMD3100 group, while compared with the LIPUS + hAD-MSCs group, the AMH level was significantly lower in the LIPUS + hAD-MSCs + AMD3100 group, from the third week after hAD-MSC transplantation ( $P < 0.05$ , Fig. 9F).

Reproductive capacity of rats was detected by mating trials. Compared with the control group, the number of offspring was significantly lower in the POI group ( $P < 0.01$ , Fig. 9I and J), while compared with the POI group, the number of offspring was significantly greater in the hAD-MSCs, LIPUS + hAD-MSCs, hAD-MSCs + AMD3100, and LIPUS + hAD-MSCs + AMD3100 groups ( $P < 0.05$ , Fig. 9I and J). Moreover, compared with the hAD-MSCs group, the number of offspring was significantly lower in the hAD-MSCs + AMD3100 group ( $P < 0.05$ , Fig. 9I and J), while compared with the LIPUS + hAD-MSCs group, the number of offspring was significantly lower in the LIPUS + hAD-MSCs + AMD3100 group ( $P < 0.05$ , Fig. 9I and J).

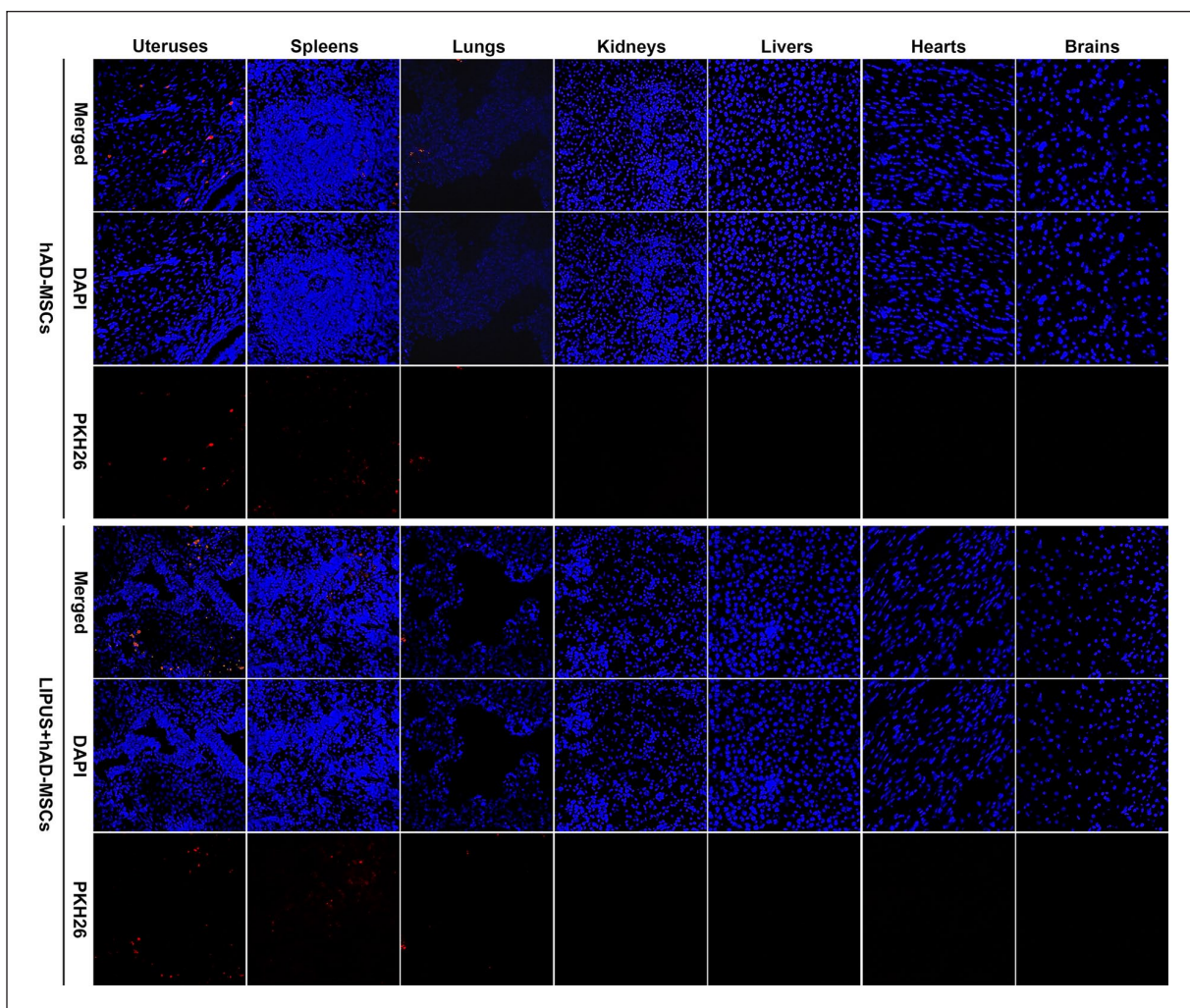


**Figure 8.** Tracking of hAD-MSCs in other important organs in rats. Transplanted PKH26-labeled hAD-MSCs were observed at 24 h after cell transplantation in the uteruses, spleens, lungs, kidneys, livers, hearts and brains of Sprague-Dawley rats in the hAD-MSCs and LIPUS + hAD-MSCs groups under a fluorescent microscope (100×00-MSCs groups under a fluorescent DAPI: 2-(4-amidinophenyl)-6-indolecarbamide dihydrochloride; hAD-MSCs: human amnion-derived mesenchymal stem cells; LIPUS: low-intensity pulsed ultrasound).

However, there was no significant difference in ovarian histology, sex hormone levels, and reproductive capacity between hAD-MSCs and LIPUS + hAD-MSCs groups or between hAD-MSCs + AMD3100 and LIPUS + hAD-MSCs+AMD3100 groups ( $P > 0.05$ , Fig. 9A–J).

These results demonstrate that both hAD-MSC and LIPUS-pretreated hAD-MSC transplantation can reduce ovarian injuries and improve ovarian function in rats with POI. The CXCR4 antagonist can reduce the number of hAD-MSCs and LIPUS-pretreated hAD-MSCs homing to the chemotherapy-induced POI ovaries, and further lessen their efficacy in POI treatment.

## Discussion

POI can cause multiple sequelae and is currently incurable. Our previous studies have demonstrated that systemically intravenously transplanted hAD-MSCs can partly reduce

ovarian injury and improve ovarian function in rats with POI<sup>8</sup>. Intravenous infusion is one of the major routes used for stem cell transplantation in regenerative medicine and tissue engineering for its minimal invasion. However, the homing rate of transplanted stem cells by intravenous infusion may be low and they arriving at the target tissue may be a small part<sup>12,27,47</sup>. The clinical application of MSC transplantation is limited by the low efficiency of cell homing *in vivo*<sup>10,11,27</sup>. Thus, how to target systemically transplanted stem cells to injured tissue with high efficiency is still a critical unsolved problem for stem cell therapy. In our previous studies, we found that the homing rate of the intravenous transplantation of hAD-MSCs to treat POI was low<sup>9</sup>, which may limit the efficiency of MSCs for POI treatment, and these results are consistent with other studies<sup>17,18</sup>. Thus, in this study, we explored methods to promote MSC homing to ovaries in systemic intravenous transplantation for POI treatment.

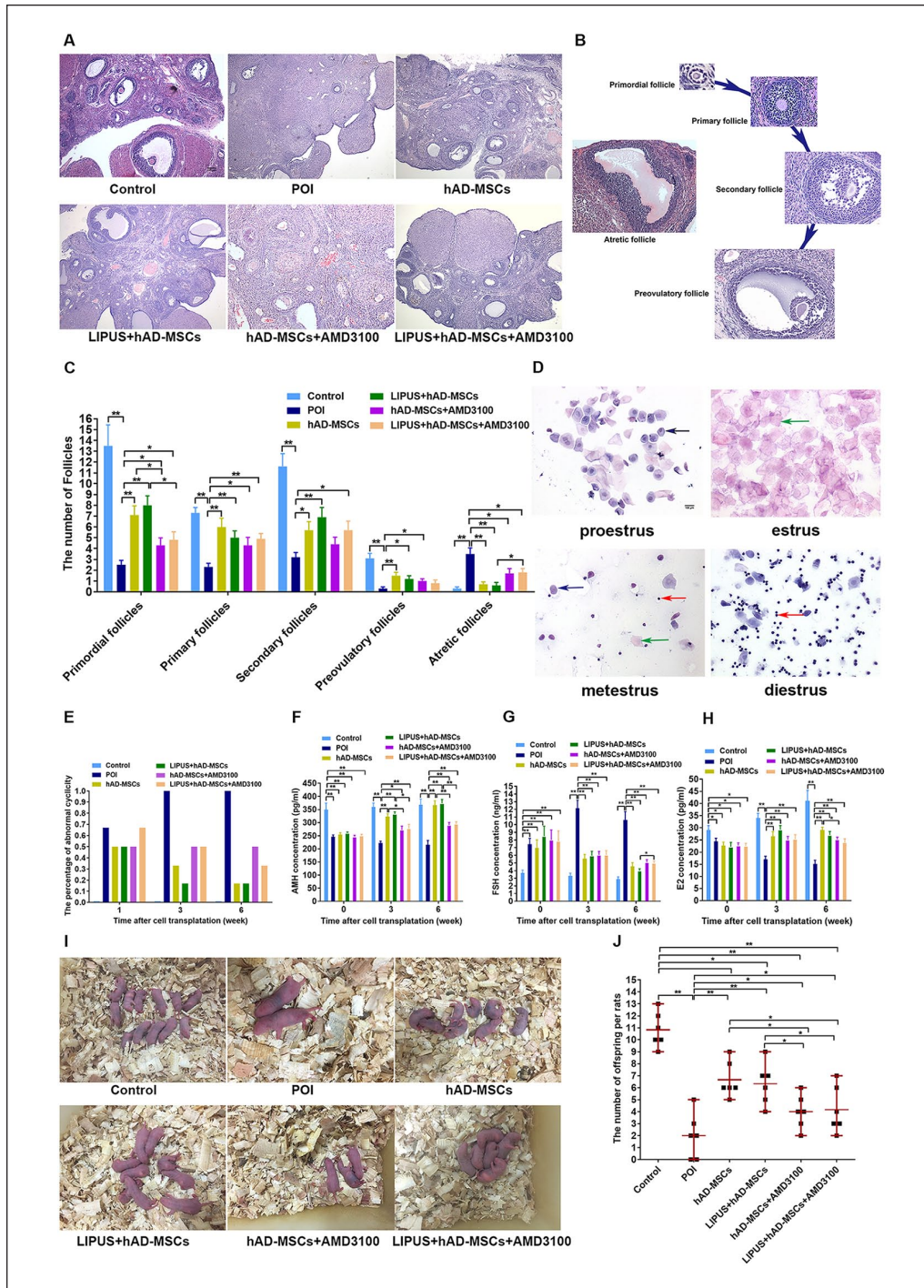


**Figure 9.** Changes in ovarian injuries and function after hAD-MSC and LIPUS-pretreated hAD-MSC transplantation in chemotherapy-induced POI rats. (A) Histological changes of ovaries were analyzed by hematoxylin and eosin staining in the control, POI, hAD-MSCs, LIPUS + hAD-MSCs, hAD-MSCs + AMD3100, and LIPUS + hAD-MSCs + AMD3100 groups (40×0D (B) The morphology of follicles at different stages was shown. (C) The number of follicles at different stages was counted and compared at 6 weeks after cell transplantation in the six groups (n = 10). (D, E) The estrous cycle of Sprague-Dawley rats, consisting of four sequential stages, proestrus, estrus, metestrus, and diestrus, was shown (D) (200×00quential stages, proestrus, estrus, metestrus, and diestrus, was shown (D) (I, 3, and 6 weeks after hAD-MSC transplantation in the six groups (n = 6). (F–H) Serum levels of (F) AMH, (G) FSH and (H) E2 were tested at 0, 3, and 6 weeks after hAD-MSC transplantation in the six groups (n = 6). (I, J) The number of offspring per rats in each group was recorded (I) and compared (J) (n = 6). Representative images are shown. The blue arrows indicate nucleated epithelial cells, the green arrows indicate cornified epithelium, and the red arrows indicate leukocytes. One-way analysis of variance was used for multiple-group comparisons. AMH: anti-Müllerian hormone; FSH: follicle-stimulating hormone; hAD-MSCs: human amnion-derived mesenchymal stem cells; LIPUS: low-intensity pulsed ultrasound; POI: premature ovarian insufficiency. \**P* < 0.05; \*\**P* < 0.01. Scale bars = 100 μ0.

Primary MSCs that have undergone three or four passages, which reach high purity, are typically evaluated for matching the international Society of Cell Therapy (ISCT) criteria for MSCs<sup>48</sup>. With the increase of MSC passage number *in vitro*, telomere length shortens after each cell division cycle, which leads to gradual senescence of MSCs and further influences the function and survival of MSCs<sup>49</sup>. hAD-MSCs have been demonstrated to not only have the features of MSCs but also have the great advantages over other stem cells<sup>5-8</sup>. Thus, hAD-MSCs were selected for this study. In this study, to identify whether P5 of hAD-MSCs underwent senescence, we compared P5 with P3 of hAD-MSCs in cell growth and senescence. SA- $\beta$ -gal of hAD-MSCs in cell growth and senescence study, to *i*<sup>43</sup>. p16 and p21 are considered as biomarkers of MSC senescence<sup>43</sup>. Zhang et al.<sup>45</sup> revealed that Ndufs6 played a critical role in the regulation of BM-MSC senescence, and downregulation of Ndufs6 accelerated BM-MSC senescence. Zhang et al.<sup>44</sup> reported that Rap1 deficiency enhanced self-renewal and delayed senescence in human MSCs. Interestingly, Ding et al.<sup>50</sup> found that Rap1 was also essential to maintain the paracrine action and immunomodulatory function of MSCs. In our study, it was found that there was no significant difference in the cell growth, expressions of p16, p21, Ndufs6 and Rap1, and hAD-MSC senescence rates between P3 and P5 of hAD-MSCs. The results demonstrate that the hAD-MSCs at P5 have not yet undergone significant senescence and hypofunction due to *in vitro* replication expansion and are able to be used for subsequent transplantation therapy.

Although the cellular mechanisms that direct the homing of MSCs are only partially understood, studies have found that some specific chemokine receptors are typically associated with MSC migration and homing<sup>19,24,25</sup>. A number of studies have demonstrated that locally elevated chemokine concentration in tissue, acting via its specific chemokine receptor on MSCs, is critical for MSCs homing to injured tissue, including bone marrow, infarcted myocardium, traumatic brain, and injured liver and lymphoid organs<sup>26,27,32,51,52</sup>. In our study, we firstly proved that hAD-MSCs expressed these chemokine receptors, including CCR1, CCR2, CCR3, CCR4, CCR5, CCR7, CCR9, CCR10, CXCR1, CXCR2, CXCR4, CXCR5, CXCR6, and CX3CR1. Thus, we speculated whether there were methods to promote the expression of these chemokine receptors, which might promote MSC migration and homing.

LIPUS is a form of mechanical vibration energy transmission with low-intensity and low thermal effect, with minimal or no adverse effects on cells<sup>53</sup>. The acoustic pressure wave generated by LIPUS is able to transmit into and/or through living cells, and leads to a series of biochemical events at the cellular level<sup>33,34</sup>. In our study, we demonstrate that LIPUS can promote the viability and proliferation of hAD-MSCs, and does not increase the apoptosis of hAD-MSCs.

Bandow et al.<sup>54</sup> found that LIPUS can induce the expression of chemokines in osteoblasts, which benefited cell

migration. Wei et al.<sup>24</sup> found that LIPUS can upregulate CXCR4 expression in BM-MSCs and promote BM-MSC migration to fracture site. Xiao et al.<sup>39</sup> found that the expression of CCR2 and CXCR4 was elevated by LIPUS stimulation in bone marrow stromal cells (BMSCs) and LIPUS was able to activate and improve migration of BMSCs. In this study, we also demonstrate that LIPUS can promote the expression of chemokine receptors in hAD-MSCs, especially the expression of CXCR4.

Some studies have found that chemokines, released from tissue, and chemokine receptors, expressed on MSCs, may partly mediate MSC actively homing to specific sites and subsequent retention in tissue<sup>19</sup>. SDF-1, a CXC chemokine family member, secreted by certain tissue and cells after injury, has been demonstrated to attract MSCs via its receptor, CXCR4, found on the cell surface of MSCs, and mobilize stem cells into injured tissue<sup>55-60</sup>. Expression of SDF-1, which is low under basal conditions, increases in inflammation, infarction, and tumor and injury tissue<sup>61-65</sup>. Previous researches showed that SDF-1 expression up-regulation after myocardial infarction mainly enhanced retention of transplanted MSCs in the injured myocardium<sup>66,67</sup>. Kitaori et al.<sup>68</sup> found that SDF-1 level was elevated in the fracture site, which recruited MSCs homing to the site of injured bone and promoted bone repair. In our study, we found the significantly elevated expression of SDF-1 in ovaries in POI rats induced by chemotherapy, which is consistent with other studies<sup>65</sup>. Some studies<sup>24,69</sup> found that MSCs expressed CXCR4 and SDF-1/CXCR4 axis was critical for the recruitment of MSCs to the injured tissue. Wei et al.<sup>24</sup> found that SDF-1/CXCR4 axis played a very important role in the LIPUS-promoted BM-MSC migration to fracture site. Thus, we speculated that the upregulated SDF-1 levels in ovaries of POI rats might regulate the migration and homing of transplanted hAD-MSCs, which express CXCR4, from the systemic circulation to ovaries, and LIPUS can promote CXCR4 expression in hAD-MSCs, which might increase the homing of infused LIPUS-pretreated hAD-MSCs to POI ovaries through SDF-1/CXCR4 axis.

To confirm our speculation, we firstly explored the effects of SDF-1 on hAD-MSC migration and the effects of LIPUS on hAD-MSC migration induced by SDF-1 *in vitro*. We found that SDF-1 can induce hAD-MSC migration and LIPUS treatment can promote hAD-MSC migration induced by SDF-1 through SDF-1/CXCR4 axis *in vitro*. Cell migration is an important part of cell homing<sup>13,14</sup>. These results indicate that pretreating hAD-MSCs with LIPUS might increase the number of hAD-MSCs homing to the ovaries with elevated SDF-1 levels in rats with chemotherapy-induced POI and the subsequent confirmation experiments were done. We demonstrate that ovaries of chemotherapy-induced POI rats are able to attract hAD-MSCs and LIPUS-pretreated hAD-MSCs, and the direct interaction of CXCR4 on hAD-MSCs with SDF-1 in ovaries plays an important role in the homing of hAD-MSCs to POI ovaries. Pretreating

hAD-MSCs with LIPUS can increase the number of hAD-MSCs homing to the ovaries of POI rats to some extent. However, the difference was not significant.

In this study, we found that LIPUS can promote CXCR4 expression in hAD-MSCs and further promote hAD-MSC migration induced by SDF-1 through SDF-1/CXCR4 axis *in vitro*. However, the efficacy of LIPUS in promoting the homing of hAD-MSCs to chemotherapy-induced POI ovaries *in vivo* was not satisfactory. Some factors and limitations of this study might be responsible for the results. First, the efficacy of LIPUS may be actually not significant. Second, PKH26 Red Fluorescent Cell Linker Kit used to track and locate the transplanted hAD-MSCs in rats is probably less sensitive than the near-infrared (NIR) dye carbocyanine 1,1-dioctadecyl-3,3,3,3 tetramethylindotricarbocyanine iodide (DiR)<sup>70</sup> or Luciferase<sup>71</sup> for *in vivo* imaging, which might influence the observation and quantification of the distribution of hAD-MSCs in ovaries and other organs of POI rats. Third, the technique<sup>19</sup> used to quantify the number of hAD-MSCs might have deviation, which is not able to accurately calculate the number of hAD-MSCs in the whole ovaries and other organs limited by current technology. Fourth, the I<sub>SATA</sub> and ET of LIPUS selected in this study are possibly not the most appropriate parameters to promote hAD-MSC homing to POI ovaries, which might influence the efficacy of LIPUS treatment. All of these problems will be improved in our follow-up research. In addition, although hAD-MSCs may be a promising *seed cell* for regenerative medicine, studies have found that there are scalability and interdonor variability associated with primary donor-derived MSC production<sup>72,73</sup>, which might also influence the results of our experiments. Thus, in our future study, hAD-MSCs should be manufactured under Good Manufacturing Practice (GMP) conditions and a rigorous quality control system of hAD-MSCs must be established to reduce the influence of those problems<sup>74</sup>. Moreover, some studies found that induced pluripotent stem cell (iPSC)-derived MSCs might overcome the disadvantages of primary donor-derived MSCs mentioned above<sup>72,73</sup>, which might provide a new direction to explore for the improvement of the experiments.

Although pretreating hAD-MSCs with LIPUS only increased the number of hAD-MSCs homing to the ovaries of POI rats to some extent, our previous studies have demonstrated that compared with hAD-MSC transplantation, LIPUS-pretreated hAD-MSC transplantation is more advantageous for reducing inflammation, improving the local microenvironment, and inhibiting granulosa cell apoptosis induced by chemotherapy in ovaries of POI rats<sup>40</sup>, which might be partly due to the increased number of hAD-MSCs homing to POI ovaries promoted by LIPUS treatment. On the contrary, the results in this study further demonstrated that both hAD-MSC and LIPUS-pretreated hAD-MSC transplantation reduced ovarian injuries and improved ovarian function in rats with POI, and the CXCR4 antagonist reduced

the number of hAD-MSCs and LIPUS-pretreated hAD-MSCs homing to the POI ovaries, and thus lessened their efficacy in POI treatment. Therefore, exploration of methods to promote MSC homing is necessary. Enhancing MSC homing to specific tissue is more likely to achieve a therapeutic effect required for disease and might provide better outcomes for patients.<sup>10,12</sup>

## Conclusion

LIPUS can promote the expression of chemokine receptors in hAD-MSCs. The LIPUS can promote CXCR4 expression in hAD-MSCs and further promote hAD-MSC migration induced by SDF-1 through SDF-1/CXCR4 axis *in vitro*. Chemokine receptor, CXCR4, expressed in hAD-MSCs, may play an important role in the migration and homing of systemically transplanted hAD-MSCs and LIPUS-pretreated hAD-MSCs to chemotherapy-induced POI ovaries in rats. Pretreating hAD-MSCs with LIPUS can increase the number of hAD-MSCs homing to the ovaries of POI rats to some extent. However, the difference is not significant and further investigation is still needed. Pretreating MSCs with LIPUS before transplantation might provide a novel, convenient, and safe technique to explore for improving the homing of systemically transplanted MSCs to target tissue.

## Acknowledgments

We thank the State Key Laboratory of Ultrasound Engineering in Medicine Co-founded by Chongqing and the Ministry of Science and Technology, Chongqing Key Laboratory of Biomedical Engineering and Laboratory of Stem Cell and Tissue Engineering of Chongqing Medical University for their technical assistance.

## Author Contributions

Conceived and designed the experiments: LL

Literature search: LL, JYH, HS, YBH.

Performed the experiments: LL, JYH, HS, YBH.

Analyzed the data: LL, JYH.

Helped perform the analysis with constructive discussions: LL, YW, JYH.

Drafted the manuscript: LL.

All authors read and approved the final manuscript.

## Availability of Data and Materials

All data generated and/or analyzed during this study are included in this published article.

## Ethical Approval

The research was in compliance with the Helsinki Declaration and approved by the Ethics Committee of the Second Affiliated Hospital of Chongqing Medical University. Animal experimental protocols were approved by the Ethics Committee of the Second Affiliated Hospital of Chongqing Medical University. Permit number: 2016-044.



## Statement of Human and Animal Rights

The experimental protocol relating to human and rats was in accordance with the US National Institutes of Health's Guidelines of Laboratory Animal Use and approved by the Ethics Committee of the Second Affiliated Hospital of Chongqing Medical University.

## Statement of Informed Consent

Written informed consent was obtained from all donors before collecting amnion for their anonymized information to be published in this article.

## Declaration of Conflicting Interests

The author(s) declared no potential conflicts of interest with respect to the research, authorship, and/or publication of this article.

## Funding

The author(s) disclosed receipt of the following financial support for the research, authorship, and/or publication of this article: This work was supported by the National Natural Science Foundation of China (No.81671415), Natural Science Foundation of Chongqing (No. cstc2019jcyj-msxmX0850), Chongqing Medical Scientific Research Project (Joint Project of Chongqing Health Commission and Science and Technology Bureau) (No. 2021MSXM061) and Basic Research and Frontier Exploration Project of Yuzhong District, Chongqing (No. 20210133).

## ORCID iD

Li Ling  <https://orcid.org/0000-0001-7712-3277>

## References

1. European Society for Human Reproduction and Embryology (ESHRE) Guideline Group on POI, Webber L, Davies M, Anderson R, Bartlett J, Braat D, Cartwright B, Cifkova R, de Muinck Keizer-Schrama S, Hogervorst E, Janse F, et al. ESHRE guideline: management of women with premature ovarian insufficiency. *Hum Reprod.* 2016;31(5):926–37.
2. Karp JM, Leng Teo GS. Mesenchymal stem cell homing: the devil is in the details. *Cell Stem Cell.* 2009;4(3):206–16.
3. Takahashi A, Yousif A, Hong L, Chefetz I. Premature ovarian insufficiency: pathogenesis and therapeutic potential of mesenchymal stem cell. *J Mol Med (Berlin).* 2021;99(5):637–50.
4. He Y, Chen D, Yang L, Hou Q, Ma H, Xu X. The therapeutic potential of bone marrow mesenchymal stem cells in premature ovarian failure. *Stem Cell Res Ther.* 2018;9(1):263.
5. Liu QW, Huang QM, Wu HY, Zuo GS, Gu HC, Deng KY, Xin HB. Characteristics and therapeutic potential of human amnion-derived stem cells. *Int J Mol Sci.* 2021;22(2):970.
6. Ling L, Wei T, He L, Wang Y, Wang Y, Feng X, Zhang W, Xiong Z. Low-intensity pulsed ultrasound activates ERK1/2 and PI3K-Akt signalling pathways and promotes the proliferation of human amnion-derived mesenchymal stem cells. *Cell Prolif.* 2017;50(6):e12383.
7. Parolini O, Alviano F, Bagnara GP, Bilic G, Buhring HJ, Evangelista M, Hennerbichler S, Liu B, Magatti M, Mao N, Miki T, et al. Concise review: isolation and characterization of cells from human term placenta: outcome of the first international Workshop on Placenta Derived Stem Cells. *Stem Cells.* 2008;26(2):300–11.
8. Ling L, Feng X, Wei T, Wang Y, Wang Y, Wang Z, Tang D, Luo Y, Xiong Z. Human amnion-derived mesenchymal stem cell (hAD-MSC) transplantation improves ovarian function in rats with premature ovarian insufficiency (POI) at least partly through a paracrine mechanism. *Stem Cell Res Ther.* 2019;10(1):46.
9. Feng X, Ling L, Zhang W, Liu X, Wang Y, Luo Y, Xiong Z. Effects of human amnion-derived mesenchymal stem Cell (hAD-MSC) transplantation in situ on primary ovarian insufficiency in SD rats. *Reprod Sci.* 2020;27(7):1502–12.
10. Fu Y, Ni J, Chen J, Ma G, Zhao M, Zhu S, Shi T, Zhu J, Huang Z, Zhang J, Chen J. Dual-functionalized MSCs that express CX3CR1 and IL-25 exhibit enhanced therapeutic effects on inflammatory bowel disease. *Mol Ther.* 2020;28(4):1214–28.
11. Wang X, Wu J, Ma S, Xie Y, Liu H, Yao M, Zhang Y, Yang GL, Yang B, Guo R, Guan F. Resveratrol preincubation enhances the therapeutic efficacy of hUC-MSCs by improving cell migration and modulating neuroinflammation mediated by MAPK signaling in a mouse model of Alzheimer's disease. *Front Cell Neurosci.* 2020;14:62.
12. Croft AS, Illien-Junger S, Grad S, Guerrero J, Wangler S, Gantenbein B. The application of mesenchymal stromal cells and their homing capabilities to regenerate the intervertebral disc. *Int J Mol Sci.* 2021;22(7):3519.
13. Sohni A, Verfaillie CM. Mesenchymal stem cells migration homing and tracking. *Stem Cells Int.* 2013;2013:130763.
14. Chen J, Jiang J, Wang W, Qin J, Chen J, Chen W, Wang Y. Low intensity pulsed ultrasound promotes the migration of bone marrow-derived mesenchymal stem cells via activating FAK-ERK1/2 signalling pathway. *Artif Cells Nanomed Biotechnol.* 2019;47(1):3603–13.
15. Wu J, Sun Z, Sun HS, Wu J, Weisel RD, Keating A, Li ZH, Feng ZP, Li RK. Intravenously administered bone marrow cells migrate to damaged brain tissue and improve neural function in ischemic rats. *Cell Transplant.* 2008;16(10):993–1005.
16. Walczak P, Zhang J, Gilad AA, Kedziorek DA, Ruiz-Cabello J, Young RG, Pittenger MF, van Zijl PC, Huang J, Bulte JW. Dual-modality monitoring of targeted intraarterial delivery of mesenchymal stem cells after transient ischemia. *Stroke.* 2008;39(5):1569–74.
17. Xiao GY, Liu IH, Cheng CC, Chang CC, Lee YH, Cheng WT, Wu SC. Amniotic fluid stem cells prevent follicle atresia and rescue fertility of mice with premature ovarian failure induced by chemotherapy. *PLoS ONE.* 2014;9(9):e106538.
18. Lai D, Wang F, Yao X, Zhang Q, Wu X, Xiang C. Human endometrial mesenchymal stem cells restore ovarian function through improving the renewal of germline stem cells in a mouse model of premature ovarian failure. *J Transl Med.* 2015;13:155.
19. Belema-Bedada F, Uchida S, Martire A, Kostin S, Braun T. Efficient homing of multipotent adult mesenchymal stem cells depends on FROUNT-mediated clustering of CCR2. *Cell Stem Cell.* 2008;2(6):566–75.
20. Ji JF, He BP, Dheen ST, Tay SS. Interactions of chemokines and chemokine receptors mediate the migration of mesenchymal stem cells to the impaired site in the brain after hypoglossal nerve injury. *Stem Cells.* 2004;22(3):415–27.

21. Li L, Lim RZL, Lee LSU, Chew NSY. HIV glycoprotein gp120 enhances mesenchymal stem cell migration by upregulating CXCR4 expression. *Biochim Biophys Acta Gen Subj*. 2018;1862(8):1790–800.
22. Won YW, Patel AN, Bull DA. Cell surface engineering to enhance mesenchymal stem cell migration toward an SDF-1 gradient. *Biomaterials*. 2014;35(21):5627–35.
23. Wang X, Wang C, Gou W, Xu X, Wang Y, Wang A, Xu W, Guo Q, Liu S, Lu Q, Meng H, et al. The optimal time to inject bone mesenchymal stem cells for fracture healing in a murine model. *Stem Cell Res Ther*. 2018;9(1):272.
24. Wei FY, Leung KS, Li G, Qin J, Chow SK, Huang S, Sun MH, Qin L, Cheung WH. Low intensity pulsed ultrasound enhanced mesenchymal stem cell recruitment through stromal derived factor-1 signaling in fracture healing. *PLoS ONE*. 2014;9(9):e106722.
25. Sordi V, Malosio ML, Marchesi F, Mercalli A, Melzi R, Giordano T, Belmonte N, Ferrari G, Leone BE, Bertuzzi F, Zerbini G, et al. Bone marrow mesenchymal stem cells express a restricted set of functionally active chemokine receptors capable of promoting migration to pancreatic islets. *Blood*. 2005;106(2):419–27.
26. Guo YC, Chiu YH, Chen CP, Wang HS. Interleukin-1beta induces CXCR3-mediated chemotaxis to promote umbilical cord mesenchymal stem cell transendothelial migration. *Stem Cell Res Ther*. 2018;9(1):281.
27. Li H, Jiang Y, Jiang X, Guo X, Ning H, Li Y, Liao L, Yao H, Wang X, Liu Y, Zhang Y, et al. CCR7 guides migration of mesenchymal stem cell to secondary lymphoid organs: a novel approach to separate GvHD from GvL effect. *Stem Cells*. 2014;32(7):1890–903.
28. Cheng Z, Ou L, Zhou X, Li F, Jia X, Zhang Y, Liu X, Li Y, Ward CA, Melo LG, Kong D. Targeted migration of mesenchymal stem cells modified with CXCR4 gene to infarcted myocardium improves cardiac performance. *Mol Ther*. 2008;16(3):571–79.
29. Yu SP, Wei Z, Wei L. Preconditioning strategy in stem cell transplantation therapy. *Transl Stroke Res*. 2013;4(1):76–88.
30. Maeda A. Recruitment of mesenchymal stem cells to damaged sites by plant-derived components. *Front Cell Dev Biol*. 2020;8:437.
31. Zamani M, Prabhakaran MP, Thian ES, Ramakrishna S. Controlled delivery of stromal derived factor-1alpha from poly lactic-co-glycolic acid core-shell particles to recruit mesenchymal stem cells for cardiac regeneration. *J Colloid Interface Sci*. 2015;451:144–52.
32. Ghadge SK, Muhlstedt S, Ozcelik C, Bader M. SDF-1alpha as a therapeutic stem cell homing factor in myocardial infarction. *Pharmacol Ther*. 2011;129(1):97–108.
33. Padilla F, Puts R, Vico L, Raum K. Stimulation of bone repair with ultrasound: a review of the possible mechanic effects. *Ultrasonics*. 2014;54(5):1125–45.
34. Hu B, Zhang Y, Zhou J, Li J, Deng F, Wang Z, Song J. Low-intensity pulsed ultrasound stimulation facilitates osteogenic differentiation of human periodontal ligament cells. *PLoS ONE*. 2014;9(4):e95168.
35. Lv Y, Zhao P, Chen G, Sha Y, Yang L. Effects of low-intensity pulsed ultrasound on cell viability, proliferation and neural differentiation of induced pluripotent stem cells-derived neural crest stem cells. *Biotechnol Lett*. 2013;35(12):2201–12.
36. Wang X, Lin Q, Zhang T, Wang X, Cheng K, Gao M, Xia P, Li X. Low-intensity pulsed ultrasound promotes chondrogenesis of mesenchymal stem cells via regulation of autophagy. *Stem Cell Res Ther*. 2019;10(1):41.
37. Harrison A, Lin S, Pounder N, Mikuni-Takagaki Y. Mode & mechanism of low intensity pulsed ultrasound (LIPUS) in fracture repair. *Ultrasonics*. 2016;70:45–52.
38. Wang J, Wang CD, Zhang N, Tong WX, Zhang YF, Shan SZ, Zhang XL, Li QF. Mechanical stimulation orchestrates the osteogenic differentiation of human bone marrow stromal cells by regulating HDAC1. *Cell Death Dis*. 2016;7:e2221.
39. Xiao W, Xu Q, Zhu Z, Li L, Chen W. Different performances of CXCR4, integrin-1beta and CCR-2 in bone marrow stromal cells (BMSCs) migration by low-intensity pulsed ultrasound stimulation. *Biomed Tech (Berlin)*. 2017;62(1):89–95.
40. Ling L, Feng X, Wei T, Wang Y, Wang Y, Zhang W, He L, Wang Z, Zeng Q, Xiong Z. Effects of low-intensity pulsed ultrasound (LIPUS)-pretreated human amnion-derived mesenchymal stem cell (hAD-MSC) transplantation on primary ovarian insufficiency in rats. *Stem Cell Res Ther*. 2017;8(1):283.
41. Mitchell B, Peel S. *Histology*, 1st ed. [London (UK)]: Churchill Livingstone; 2009.
42. Wang Z, Wang Y, Yang T, Li J, Yang X. Study of the reparative effects of menstrual-derived stem cells on premature ovarian failure in mice. *Stem Cell Res Ther*. 2017;8(1):11.
43. Liu J, Ding Y, Liu Z, Liang X. Senescence in mesenchymal stem cells: functional alterations, molecular mechanisms, and rejuvenation strategies. *Front Cell Dev Biol*. 2020;8:258.
44. Zhang X, Liu Z, Liu X, Wang S, Zhang Y, He X, Sun S, Ma S, Shyh-Chang N, Liu F, Wang Q, et al. Telomere-dependent and telomere-independent roles of RAP1 in regulating human stem cell homeostasis. *Protein Cell*. 2019;10(9):649–67.
45. Zhang Y, Guo L, Han S, Chen L, Li C, Zhang Z, Hong Y, Zhang X, Zhou X, Jiang D, Liang X, et al. Adult mesenchymal stem cell ageing interplays with depressed mitochondrial Ndufs6. *Cell Death Dis*. 2020;11(12):1075.
46. Ling L, Hou J, Liu D, Tang D, Zhang Y, Zeng Q, Pan H, Fan L. Important role of the SDF-1/CXCR4 axis in the homing of systemically transplanted human amnion-derived mesenchymal stem cells (hAD-MSCs) to ovaries in rats with chemotherapy-induced premature ovarian insufficiency (POI). *Stem Cell Res Ther*. 2022;13(1):79.
47. Lee RH, Pulin AA, Seo MJ, Kota DJ, Ylostalo J, Larson BL, Semprun-Prieto L, Delafontaine P, Prockop DJ. Intravenous hMSCs improve myocardial infarction in mice because cells embolized in lung are activated to secrete the anti-inflammatory protein TSG-6. *Cell Stem Cell*. 2009;5(1):54–63.
48. Samsonraj RM, Raghunath M, Nurcombe V, Hui JH, van Wijnen AJ, Cool SM. Concise review: multifaceted characterization of human mesenchymal stem cells for use in regenerative medicine. *Stem Cells Transl Med*. 2017;6(12):2173–85.
49. He F, Yu C, Liu T, Jia H. Ginsenoside Rg1 as an effective regulator of mesenchymal stem cells. *Front Pharmacol*. 2019;10:1565.
50. Ding Y, Liang X, Zhang Y, Yi L, Shum HC, Chen Q, Chan BP, Fan H, Liu Z, Tergaonkar V, Qi Z, et al. Rap1 deficiency-provoked paracrine dysfunction impairs immunosuppressive potency of mesenchymal stem cells in allograft rejection of heart transplantation. *Cell Death Dis*. 2018;9(3):386.
51. Ma J, Liu N, Yi B, Zhang X, Gao BB, Zhang Y, Xu R, Li X, Dai Y. Transplanted hUCB-MSCs migrated to the damaged area by SDF-1/CXCR4 signaling to promote functional recovery after traumatic brain injury in rats. *Neurol Res*. 2015;37(1):50–56.

52. Xiao Ling K, Peng L, Jian Feng Z, Wei C, Wei Yan Y, Nan S, Cheng Qi G, Zhi Wei W. Stromal derived factor-1/CXCR4 axis involved in bone marrow mesenchymal stem cells recruitment to injured liver. *Stem Cells Int*. 2016;2016:8906945.
53. Bashardoust Tajali S, Houghton P, MacDermid JC, Grewal R. Effects of low-intensity pulsed ultrasound therapy on fracture healing: a systematic review and meta-analysis. *Am J Phys Med Rehabil*. 2012;91(4):349–67.
54. Bandow K, Nishikawa Y, Ohnishi T, Kakimoto K, Soejima K, Iwabuchi S, Kuroe K, Matsuguchi T. Low-intensity pulsed ultrasound (LIPUS) induces RANKL, MCP-1, and MIP-1beta expression in osteoblasts through the angiotensin II type I receptor. *J Cell Physiol*. 2007;211(2):392–98.
55. Zhang D, Fan GC, Zhou X, Zhao T, Pasha Z, Xu M, Zhu Y, Ashraf M, Wang Y. Over-expression of CXCR4 on mesenchymal stem cells augments myoangiogenesis in the infarcted myocardium. *J Mol Cell Cardiol*. 2008;44(2):281–92.
56. Liekens S, Schols D, Hatse S. CXCL12-CXCR4 axis in angiogenesis, metastasis and stem cell mobilization. *Curr Pharm Des*. 2010;16(35):3903–20.
57. Kavanagh DP, Kalia N. Hematopoietic stem cell homing to injured tissues. *Stem Cell Rev Rep*. 2011;7(3):672–82.
58. Jin W, Liang X, Brooks A, Futrega K, Liu X, Doran MR, Simpson MJ, Roberts MS, Wang H. Modelling of the SDF-1/CXCR4 regulated in vivo homing of therapeutic mesenchymal stem/stromal cells in mice. *PeerJ*. 2018;6:e6072.
59. Tang Q, Luo C, Lu B, Fu Q, Yin H, Qin Z, Lyu D, Zhang L, Fang Z, Zhu Y, Yao K. Thermosensitive chitosan-based hydrogels releasing stromal cell derived factor-1 alpha recruit MSC for corneal epithelium regeneration. *Acta Biomater*. 2017;61:101–13.
60. Zhang H, Li X, Li J, Zhong L, Chen X, Chen S. SDF-1 mediates mesenchymal stem cell recruitment and migration via the SDF-1/CXCR4 axis in bone defect. *J Bone Miner Metab*. 2021;39(2):126–38.
61. Pagella P, Nombela-Arrieta C, Mitsiadis TA. Distinct expression patterns of Cxcl12 in mesenchymal stem cell niches of intact and injured rodent teeth. *Int J Mol Sci*. 2021;22(6):3024.
62. Yu J, Kim HM, Kim KP, Son Y, Kim MS, Park KS. Ceramide kinase regulates the migration of bone marrow-derived mesenchymal stem cells. *Biochem Biophys Res Commun*. 2019;508(2):361–67.
63. Chen Y, Jin X, Zeng Z, Liu W, Wang B, Wang H. Estrogen-replacement therapy promotes angiogenesis after acute myocardial infarction by enhancing SDF-1 and estrogen receptor expression. *Microvasc Res*. 2009;77(2):71–77.
64. Elmadbouh I, Haider HKh, Jiang S, Idris NM, Lu G, Ashraf M. Ex vivo delivered stromal cell-derived factor-1alpha promotes stem cell homing and induces angiomyogenesis in the infarcted myocardium. *J Mol Cell Cardiol*. 2007;42(4):792–803.
65. Luo Q, Yin N, Zhang L, Yuan W, Zhao W, Luan X, Zhang H. Role of SDF-1/CXCR4 and cytokines in the development of ovary injury in chemotherapy drug induced premature ovarian failure mice. *Life Sci*. 2017;179:103–109.
66. Jiang Q, Song P, Wang E, Li J, Hu S, Zhang H. Remote ischemic postconditioning enhances cell retention in the myocardium after intravenous administration of bone marrow mesenchymal stromal cells. *J Mol Cell Cardiol*. 2013;56:1–7.
67. Abbott JD, Huang Y, Liu D, Hickey R, Krause DS, Giordano FJ. Stromal cell-derived factor-1alpha plays a critical role in stem cell recruitment to the heart after myocardial infarction but is not sufficient to induce homing in the absence of injury. *Circulation*. 2004;110(21):3300–3305.
68. Kitaori T, Ito H, Schwarz EM, Tsutsumi R, Yoshitomi H, Oishi S, Nakano M, Fujii N, Nagasawa T, Nakamura T. Stromal cell-derived factor 1/CXCR4 signaling is critical for the recruitment of mesenchymal stem cells to the fracture site during skeletal repair in a mouse model. *Arthritis Rheum*. 2009;60(3):813–23.
69. Song YL, Jiang H, Jiang NG, Jin YM, Zeng TT. Mesenchymal stem cell-platelet aggregates increased in the peripheral blood of patients with acute myocardial infarction and might depend on the stromal cell-derived factor 1/CXCR4 axis. *Stem Cells Dev*. 2019;28(24):1607–19.
70. Rojas-Torres M, Sanchez-Gomar I, Rosal-Vela A, Beltran-Camacho L, Eslava-Alcon S, Alonso-Pineiro JA, Martin-Ramirez J, Moreno-Luna R, Duran-Ruiz MC. Assessment of endothelial colony forming cells delivery routes in a murine model of critical limb threatening ischemia using an optimized cell tracking approach. *Stem Cell Res Ther*. 2022;13(1):266.
71. Guo R, Wan F, Morimatsu M, Xu Q, Feng T, Yang H, Gong Y, Ma S, Chang Y, Zhang S, Jiang Y, et al. Cell sheet formation enhances the therapeutic effects of human umbilical cord mesenchymal stem cells on myocardial infarction as a bioactive material. *Bioact Mater*. 2021;6(9):2999–3012.
72. Bloor AJC, Patel A, Griffin JE, Gillece MH, Radia R, Yeung DT, Drier D, Larson LS, Uenishi GI, Hei D, Kelly K, et al. Production, safety and efficacy of iPSC-derived mesenchymal stromal cells in acute steroid-resistant graft versus host disease: a phase I, multicenter, open-label, dose-escalation study. *Nat Med*. 2020;26(11):1720–25.
73. Lian Q, Zhang Y, Liang X, Gao F, Tse HF. Directed differentiation of human-induced pluripotent stem cells to mesenchymal stem cells. *Methods Mol Biol*. 2016;1416:289–98.
74. Zhao Q, Han Z, Wang J, Han Z. Development and investigational new drug application of mesenchymal stem/stromal cells products in China. *Stem Cells Transl Med*. 2021;10(Suppl2):S18–30.